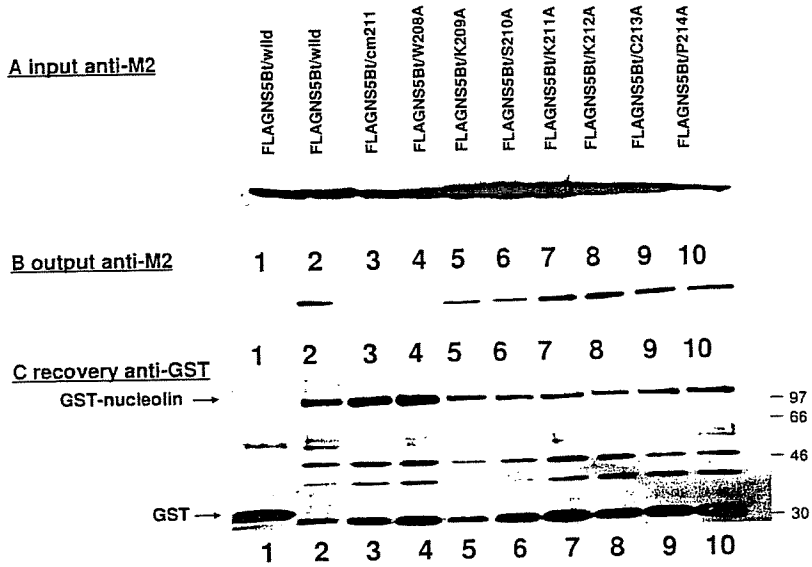

FIG. 2. Interaction between nucleolin and NS5B of HCV isolate M1LE and an essential residue for this interaction. COS1 cells were transiently cotransfected with mammalian expression vectors expressing FLAG-NS5Bt proteins (lanes: 1 and 2, wild type; 3, cm211; 4, W208A; 5, K209A; 6, S210A; 7, K211A; 8, K212A; 9, C213A; 10, P214A) and GST protein alone (lane 1) or GST-nucleolin protein (lanes 2 to 10). (A) Input of FLAG-NS5Bt proteins. Total lysates were fractionated by SDS–10% PAGE and subjected to Western blot analysis with anti-FLAG M2 monoclonal antibody. (B) Output of FLAG-NS5Bt proteins. Coprecipitants by glutathione resin were washed with PBS(−) containing 1.0% Triton X-100, fractionated by SDS–10% PAGE, and subjected to Western blot analysis with anti-FLAG M2 monoclonal antibody. (C) Recovery of GST or GST-nucleolin proteins. The nitrocellulose membrane used for Western blot analysis of coprecipitants with anti-FLAG M2 antibody was reprobed with anti-GST antibody. Molecular masses (kilodaltons) are indicated to the right of the panel.

iGENE (Tsukuba, Japan). We selected one sequence, si-Nuc, and, as a control for siRNA transfection, we utilized siRNA for luciferase (si-Luc) (GL3 luciferase duplex). Forty-eight hours after electroporation of each siRNA, at a concentration of 1 μM, into Huh7-DMB, the lysates were analyzed by Western blotting analysis with two kinds of antibody to nucleolin. We found that both anti-nucleolin antibodies detected the expression of endogenous nucleolin. Although si-Nuc efficiently knocked down the expression of endogenous nucleolin, si-Luc did not (Fig. 3), showing the specificity of the former. In addition, real-time PCR showed that si-Nuc decreased nucleolin mRNA by about one-third compared with si-Luc (data not shown).

Effect of nucleolin suppression on HCV replication. To test the effect of nucleolin knockdown on HCV RNA replication, we transfected 1 μM of si-Nuc or si-Luc along with 100 ng of replicon MA RNA into Huh7-DMB cells and selected the cells with G418. As shown in Fig. 4, we found that cotransfection of si-Nuc reduced the number of G418-resistant colonies, whereas cotransfection of si-Luc did not (Fig. 4). As a control for the efficient transfection of siRNA, we used si-HCV, which targets the HCV internal ribosome entry site and can efficiently suppress HCV replication, as described previously (51). Using this siRNA, we observed no G418-resistant colonies, indicating that siRNA was efficiently transfected under these experimental conditions. To rule out the possibility that suppression of nucleolin may have a detrimental effect on cells and may inhibit HCV RNA replication, we transfected pCI-Neo, which encodes a neomycin resistance gene under the control of a CMV promoter/enhancer, into Huh7-DMB cells, with or without si-Nuc and si-Luc, and selected the cells with 0.5 mg/dl G418. We found that the suppression of nucleolin expression did not significantly reduce the number of G418-resistant colonies (data not shown). In addition, massive cell death was not observed after the transfection of any siRNA (data not shown). These results indicate that the transient suppression of nucleolin may not affect cell proliferation but that nucleolin may affect the HCV replication complex itself.

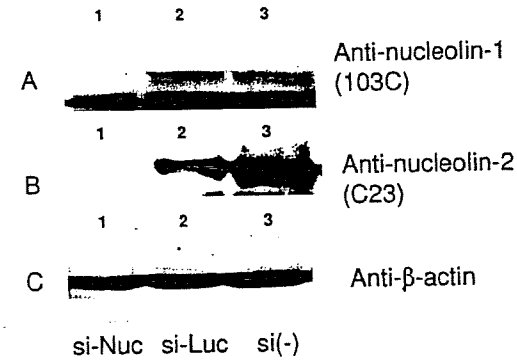

FIG. 3. Knockdown of endogenous nucleolin by siRNA. Huh7-DMB cells were electroporated with 1 μM si-Nuc and si-Luc. After 48 h, total cell lysates were fractionated by SDS–10% PAGE and subjected to Western blot analysis with the anti-nucleolin antibodies anti-nucleolin-1 (103C) in A and anti-nucleolin-2 (C23) in B and anti-β-actin antibody in C. Lanes: 1, cells transfected with si-Nuc; 2, cells transfected with si-Luc; 3, no siRNA [si(−)].

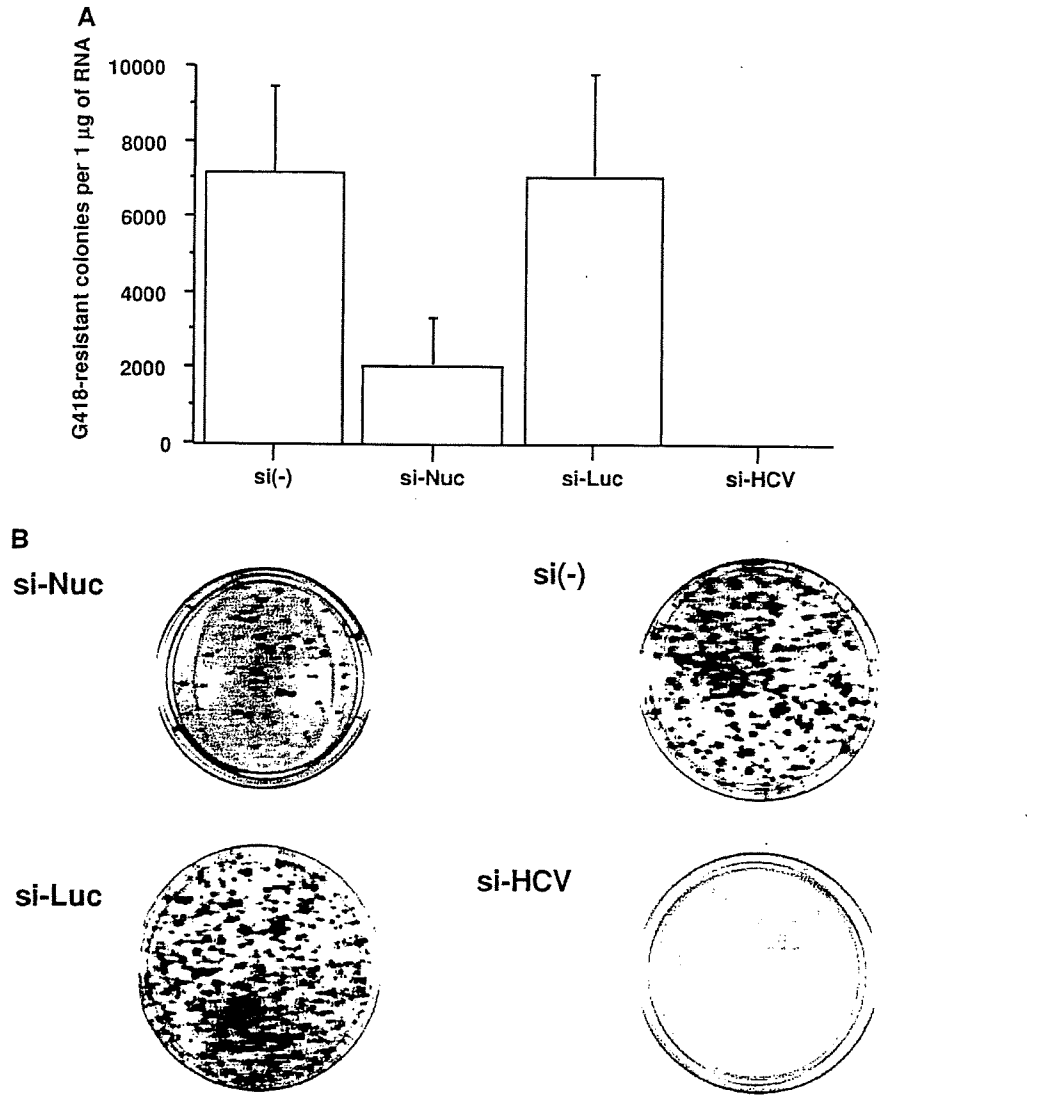

FIG. 4. Effect of suppression of endogenous nucleolin on HCV replication in the MA replicon. Huh7-DMB cells were electroporated with 1 μg of in vitro-transcribed MA RNA plus si-Nuc, si-Luc, si-HCV, or no siRNA [si(−)], and G418-resistant cells were selected with 1 mg/ml G418 and were stained 4 weeks later. (A) Mean number of G418-resistant colonies per 10-cm-diameter cell culture dish per 1 μg replicon RNA. Error bars indicate the standard deviations of the results from at least three independent experiments. (B) Visualization of G418-resistant colonies, as described in Materials and Methods.

Because the knockdown effect of siRNA does not continue for more than 3 weeks after transient transfection, the number of G418-resistant colonies may not be a good indicator of HCV RNA replication. We therefore performed a transient replication assay using a replicon in which the neomycin resistance gene was replaced by a luciferase gene, and luciferase activity was used as a marker of HCV RNA replication. Transfection of MH14 RNA, which was used as the wild-type replicon, into a subline of Huh7 cells resulted in highly efficient luciferase activity, whereas a polymerase-defective RNA replicon of MH14, MH4GHD, in which the catalytic GDD motif of NS5B polymerase was replaced by an inactive GHD motif, was used as a negative control (Fig. 5A). si-HCV and si-Luc suppressed the luciferase activity even at 24 h after transfection, but other siRNAs did not affect the luciferase activity, and luciferase activities in these siRNAs were similar to that of the control (no siRNA) at this point (Fig. 5B). We found that cotransfection of si-Nuc moderately suppressed both luciferase activity at 72 h after transfection and relative luciferase activity, whereas cotransfection of si-GFP and si-Mix did not (Fig. 5B and C). Cotransfection of si-HCV and si-Luc almost completely suppressed luciferase activity at 72 h after transfection. In a transient replication assay, the suppression of endogenous nucleolin also inhibited HCV replication.

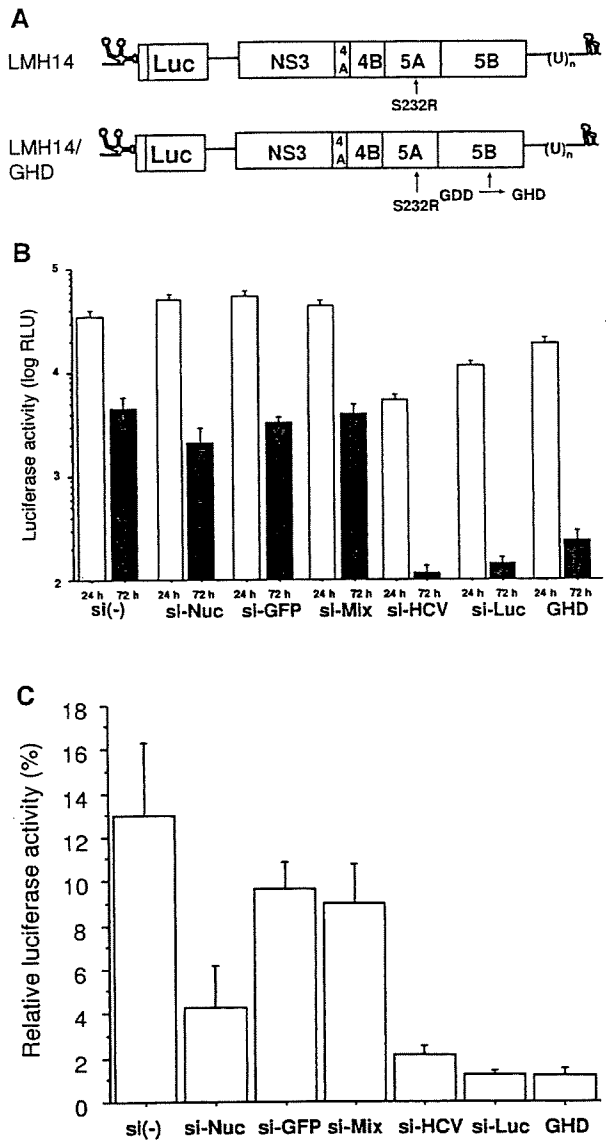

FIG. 5. Effect of suppression of endogenous nucleolin on HCV replication in the LMH14 replicon. (A) Schematic representation of the luciferase replicon. In the LMH14 replicon, the neomycin resistance gene was replaced by a luciferase gene, and S232 of NS5A was replaced by R. In the LMH14/GHD replicon, the NS5B GDD motif in LMH14 was changed to GHD and used as a negative control. (B) Cells were transfected with in vitro-transcribed LHH14 or LMH14/GHD RNA along with 2 μM of si-Mix, si-GFP, si-Nuc, si-Luc, si-HCV, or no siRNA [si(−)] using the DMRIE-C reagent, and luciferase activity (relative light units [RLU]) was measured 24 and 72 h after transfection. Shown are the activities at 24 and 72 h. Error bars indicate the standard deviations of the results from at least three independent experiments. (C) Activity at 24 h was used as an indication of each transfection. Shown are the ratios of activity (percent) at 72 h relative to that at 24 h. Error bars indicate the standard deviations of the results from at least three independent experiments.

To rule out the cytotoxic effects of the suppression of endogenous nucleolin, we transfected pGL3 control, with or without each siRNA, and measured luciferase activity 48 and 72 h after transfection. We found that cotransfection of each siRNA did not inhibit luciferase activity at both 48 and 72 h (Fig. 6), indicating that both suppression of nucleolin and transfection of siRNA did not have detrimental effects on transfected cells.

DISCUSSION

HCV replication has been found to take place in a distinctly altered membrane structure, or membranous web, of the endoplasmic reticulum (11). When HCV NS proteins are coexpressed in stable cell lines harboring replicons, they colocalize to these membrane structures, indicating that they might form a complex (16, 39, 47). These nonstructural proteins, together with host factors, form the viral replicase, the complex in which viral replication is thought to take place. The in vitro level of the RdRp activity of NS5B is low (12), indicating that cofactors, whether viral and/or host proteins and/or the appropriate cellular environment, are necessary for optimal activity of HCV RdRp. HCV NS5B has been reported to interact with NS3, NS4A, NS4B, NS5A, and NS5B itself (9, 48, 57, 65). Using an HCV subgenomic replicon, we previously reported the critical role of the interaction between NS5A and NS5B and the oligomerization of NS5B itself in HCV replication (36, 56). NS3 and NS4B have been shown to be positive and negative regulators, respectively, of NS5B in the replication complex (46).

In addition to interacting with HCV nonstructural proteins, NS5B has been reported to interact with many host proteins, including a SNARE-like protein (62); eIF4AII, an RNA-dependent ATPase/helicase; a component of the translation initiation complex (30), protein kinase C-related kinase 2, which specifically phosphorylates NS5B (27); and p68, a human RNA helicase I (15). The suppression of protein kinase C-related kinase 2 has been reported to reduce the phosphorylation of NS5B and to inhibit HCV RNA replication (27), and the suppression of p68 has been reported to inhibit the synthesis of negative-strand HCV RNA from the positive strand (15).

Several host proteins have been shown to interact with RdRp of other RNA viruses. For example, in poliovirus, an RdRp and an RdRp precursor interact with human Sam68 (38) and heterogeneous nuclear ribonucleoprotein C1/C2 (5), respectively, and modulate RdRp activity directly or indirectly. Bromo mosaic virus RdRp and tobacco mosaic virus RdRp interact with eukaryotic initiation factor 3 and eukaryotic initiation factor 3-related factor, altering RdRp activity (45, 50).

Here and in a previous report, we identified and characterized the interaction between nucleolin and HCV NS5B (20). Nucleolin was originally identified as a common phosphoprotein of growing eukaryotic cells, although its function is not completely understood. Nucleolin is a multifunctional protein that shuttles between the nucleus and cytoplasm. In addition, it is expressed on the surface of various cells, acting as a receptor for various ligands, including lipoproteins (55), cytokines, growth factors (6, 52, 60), the extracellular matrix (10, 18, 25), bacteria (58), and viruses (4, 8, 21, 41–44).

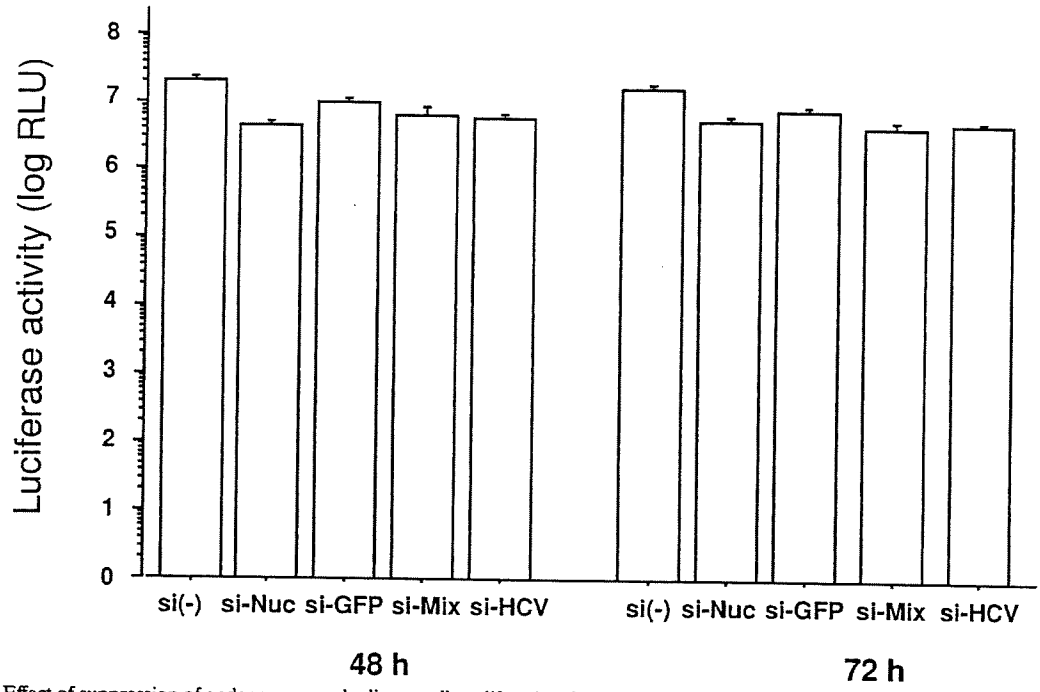

FIG. 6. Effect of suppression of endogenous nucleolin on cell proliferation. The plasmid pGL3 control, encoding the luciferase gene under the control of the CMV promoter/enhancer, was cotransfected with 2 μM of si-Mix, si-GFP, si-Nuc, si-HCV, or no siRNA [si(−)] using DMRIE-C reagent, and luciferase activity was measured 48 and 72 h after transfection. The error bars indicate the standard deviations of the results from at least three independent experiments.

We found that recombinant C-terminal nucleolin proteins can bind NS5B and inhibit its RdRp activity in a dose-dependent manner (20), suggesting that nucleolin may affect HCV replication by interacting with NS5B. The direct interaction of nucleolin with HCV NS5B in vivo and in vitro was shown to require two critical stretches of NS5B. Here, we showed that within one of these regions, aa 208 to 214, the W208 residue was critical for both binding of nucleolin and HCV replication. Transient down-regulation of endogenous nucleolin by siRNA considerably inhibited HCV replication in Huh7 cells. These results strongly indicate that nucleolin has an important role in HCV replication through its direct interaction with NS5B.

Our finding of an important positive role for nucleolin in HCV replication is apparently inconsistent with previous findings of an inhibitory role for nucleolin. It was previously reported that purified C-terminal nucleolin proteins inhibited the RdRp activity of NS5B in vitro. The latter result, however, may have been due to the use of recombinant truncated nucleolin proteins, because recombinant full-length nucleolin was not available (70). Taken together, however, these results indicate that N-terminal nucleolin may be important for the positive function of nucleolin in HCV replication, although the NS5B-binding region is within the RGG domain and RNA-binding domain 4 is at the C terminus.

Transfection of the mutant replicon containing NS5B W208A, which could not bind nucleolin, led to almost no HCV replication. By contrast, the suppression of nucleolin by siRNA moderately inhibited HCV replication, a result also observed with the transient assay using luciferase reporter replicon and G418-resistant colony formation. While HCV replication was completely inhibited by MA/W208A, replication was only partially inhibited by si-Nuc, indicating that si-Nuc can transiently suppress, but cannot eliminate, expression of endogenous nucleolin. Recently, nucleolin was reported to inhibit cell cycle progression after heat shock and genotoxic stress by increasing complex formation with human replication protein A (26). When pGL3 control or pCI-Neo was cotransfected with si-Nuc, the luciferase activity or the number of G418-resistant colonies was not reduced, strongly suggesting that the moderate inhibition of nucleolin expression did not have severe cytotoxic effects on siRNA-transfected cells. More efficient suppression of nucleolin may result in more severe inhibition of HCV RNA replication. It is therefore important to determine whether nucleolin is dispensable in mammalian cells as it is in *Saccharomyces pombe* (17) and *Saccharomyces cerevisiae* (31), since nucleolin may constitute a putative therapeutic target to inhibit HCV replication.

Using a clustered alanine substitution mutant library (CM) of NS5B, we previously showed that two stretches of NS5B amino acids, aa 208 to 214 and 500 to 506, were critical for nucleolin binding. According to the crystal models of NS5B, the former stretch is in the palm and the latter stretch is in the bottom of the thumb domain. We focused on identifying residues in aa 208 to 214 that are essential for nucleolin binding and HCV replication, as the CM mutant of aa 500 to 506 was defective in RdRp activity in vitro and HCV replication in vivo (36, 48, 49). We found that the W208 residue was critical for

both nucleolin binding and HCV replication. This residue is exposed to solvent at the edge of the palm and is not close to the catalytic pocket.

Nucleolin may stabilize monomeric NS5B, making it ready for oligomerization to NS5B, or it may facilitate the formation of a complex between NS5B and template RNA. In both cases, a substoichiometric amount of nucleolin may be required transiently at a step prior to the catalytic RdRp reaction of NS5B. Efforts to determine the contribution of amino acid residues 500 to 508 to nucleolin binding and HCV replication in vivo are ongoing and may reveal further correlations. We found that another mutant replicon, MA/K211A, reduced the number of G418-resistant colonies compared with the wild type and the other mutants. Because K211A of NS5Bt is close to the pocket of catalytic activity and did not affect binding to nucleolin, K211 may contribute to the structural integrity of the pocket or the heat-stable property of RdRp as reported previously (36).

Efficient HCV replication and infection in tissue-cultured cells by using full-length HCV RNA replicons have been reported previously (32, 63, 72). HCV replication occurs in differentiated subcellular fractions and involves dynamic complexes of structural proteins, nonstructural proteins, and HCV RNA demarcated by membrane structures. It is therefore of great interest to determine whether nucleolin is involved in such HCV-replicating intermediates in compartmented subcellular structures.

REFERENCES

1. **Alter, H. J., R. H. Purcell, J. W. Shih, J. C. Melpolder, M. Houghton, Q. L. Choo, and G. Kuo.** 1989. Detection of antibody to hepatitis C virus in prospectively followed transfusion recipients with acute and chronic non-A, non-B hepatitis. N. Engl. J. Med. 321:1494–1500.
2. **Behrens, S. E., L. Tomei, and R. De Francesco.** 1996. Identification and properties of the RNA-dependent RNA polymerase of hepatitis C virus. EMBO J. 15:12–22.
3. **Bordo, D., and P. Argos.** 1991. Suggestions for "safe" residue substitutions in site-directed mutagenesis. J. Mol. Biol. 217:721–729.
4. **Bose, S., M. Basu, and A. K. Banerjee.** 2004. Role of nucleolin in human parainfluenza virus type 3 infection of human lung epithelial cells. J. Virol. 78:8146–8158.
5. **Brunner, J. E., J. H. Nguyen, H. H. Roehl, T. V. Ho, K. M. Swiderek, and B. L. Semler.** 2005. Functional interaction of heterogeneous nuclear ribonucleoprotein C with poliovirus RNA synthesis initiation complexes. J. Virol. 79:3254–3266.
6. **Callebaut, C., S. Nisole, J. P. Briand, B. Krust, and A. G. Hovanessian.** 2001. Inhibition of HIV infection by the cytokine midkine. Virology 281:248–264.
7. **Choo, Q. L., G. Kuo, A. J. Weiner, L. R. Overby, D. W. Bradley, and M. Houghton.** 1989. Isolation of a cDNA clone derived from a blood-borne non-A, non-B viral hepatitis genome. Science 244:359–362.
8. **de Verdugo, U. R., H. C. Selinka, M. Huber, B. Kramer, J. Kellermann, P. H. Hofschneider, and R. Kandolf.** 1995. Characterization of a 100-kilodalton binding protein for the six serotypes of coxsackie B viruses. J. Virol. 69:6751–6757.
9. **Dimitrova, M., I. Imbert, M. P. Kieny, and C. Schuster.** 2003. Protein-protein interactions between hepatitis C virus nonstructural proteins. J. Virol. 77:5401–5414.
10. **Dumler, I., V. Stepanova, U. Jerke, O. A. Mayboroda, F. Vogel, P. Bouvet, V. Tkachuk, H. Haller, and D. C. Gulba.** 1999. Urokinase-induced mitogenesis is mediated by casein kinase 2 and nucleolin. Curr. Biol. 9:1468–1476.
11. **Egger, D., B. Wolk, R. Gosert, L. Bianchi, H. E. Blum, D. Moradpour, and K. Bienz.** 2002. Expression of hepatitis C virus proteins induces distinct membrane alterations including a candidate viral replication complex. J. Virol. 76:5974–5984.
12. **Ferrari, E., J. Wright-Minogue, J. W. Fang, B. M. Baroudy, J. Y. Lau, and Z. Hong.** 1999. Characterization of soluble hepatitis C virus RNA-dependent RNA polymerase expressed in *Escherichia coli*. J. Virol. 73:1649–1654.
13. **Friebe, P., and R. Bartenschlager.** 2002. Genetic analysis of sequences in the 3′ nontranslated region of hepatitis C virus that are important for RNA replication. J. Virol. 76:5326–5338.
14. **Ginisty, H., H. Sicard, B. Roger, and P. Bouvet.** 1999. Structure and functions of nucleolin. J. Cell Sci. 112:761–772.
15. **Goh, P. Y., Y. J. Tan, S. P. Lim, Y. H. Tan, S. G. Lim, F. Fuller-Pace, and W. Hong.** 2004. Cellular RNA helicase p68 relocalization and interaction with the hepatitis C virus (HCV) NS5B protein and the potential role of p68 in HCV RNA replication. J. Virol. 78:5288–5298.
16. **Gosert, R., D. Egger, V. Lohmann, R. Bartenschlager, H. E. Blum, K. Bienz, and D. Moradpour.** 2003. Identification of the hepatitis C virus RNA replication complex in Huh-7 cells harboring subgenomic replicons. J. Virol. 77:5487–5492.
17. **Gulli, M. P., J. P. Girard, D. Zabetakis, B. Lapeyre, T. Melese, and M. Caizergues-Ferrer.** 1995. gar2 is a nucleolar protein from Schizosaccharomyces pombe required for 18S rRNA and 40S ribosomal subunit accumulation. Nucleic Acids Res. 23:1912–1918.
18. **Harms, G., R. Kraft, G. Grelle, B. Volz, J. Dernedde, and R. Tauber.** 2001. Identification of nucleolin as a new L-selectin ligand. Biochem. J. 360:531–538.
19. **Hijikata, M., N. Kato, Y. Ootsuyama, M. Nakagawa, S. Ohkoshi, and K. Shimotohno.** 1991. Hypervariable regions in the putative glycoprotein of hepatitis C virus. Biochem. Biophys. Res. Commun. 175:220–228.
20. **Hirano, M., S. Kaneko, T. Yamashita, H. Luo, W. Qin, Y. Shirota, T. Nomura, K. Kobayashi, and S. Murakami.** 2003. Direct interaction between nucleolin and hepatitis C virus NS5B. J. Biol. Chem. 278:5109–5115.
21. **Hovanessian, A. G., F. Puvion-Dutilleul, S. Nisole, J. Svab, E. Perret, J. S. Deng, and B. Krust.** 2000. The cell-surface-expressed nucleolin is associated with the actin cytoskeleton. Exp. Cell Res. 261:312–328.
22. **Ikeda, M., M. Yi, K. Li, and S. M. Lemon.** 2002. Selectable subgenomic and genome-length dicistronic RNAs derived from an infectious molecular clone of the HCV-N strain of hepatitis C virus replicate efficiently in cultured Huh7 cells. J. Virol. 76:2997–3006.
23. **Kato, N., Y. Ootsuyama, H. Sekiya, S. Ohkoshi, T. Nakazawa, M. Hijikata, and K. Shimotohno.** 1994. Genetic drift in hypervariable region 1 of the viral genome in persistent hepatitis C virus infection. J. Virol. 68:4776–4784.
24. **Kato, T., T. Date, M. Miyamoto, Z. Zhao, M. Mizokami, and T. Wakita.** 2005. Nonhepatic cell lines HeLa and 293 support efficient replication of the hepatitis C virus genotype 2a subgenomic replicon. J. Virol. 79:592–596.
25. **Kibbey, M. C., B. Johnson, R. Petryshyn, M. Jucker, and H. K. Kleinman.** 1995. A 110-kD nuclear shuttling protein, nucleolin, binds to the neurite-promoting IKVAV site of laminin-1. J. Neurosci. Res. 42:314–322.
26. **Kim, K., D. D. Dimitrova, K. M. Carta, A. Saxena, M. Daras, and J. A. Borowiec.** 2005. Novel checkpoint response to genotoxic stress mediated by nucleolin-replication protein A complex formation. Mol. Cell. Biol. 25:2463–2474.
27. **Kim, S. J., J. H. Kim, Y. G. Kim, H. S. Lim, and J. W. Oh.** 2004. Protein kinase C-related kinase 2 regulates hepatitis C virus RNA polymerase function by phosphorylation. J. Biol. Chem. 279:50031–50041.
28. **Kishine, H., K. Sugiyama, M. Hijikata, N. Kato, H. Takahashi, T. Noshi, Y. Nio, M. Hosaka, Y. Miyanari, and K. Shimotohno.** 2002. Subgenomic replicon derived from a cell line infected with the hepatitis C virus. Biochem. Biophys. Res. Commun. 293:993–999.
29. **Kolykhalov, A. A., K. Mihalik, S. M. Feinstone, and C. M. Rice.** 2000. Hepatitis C virus-encoded enzymatic activities and conserved RNA elements in the 3′ nontranslated region are essential for virus replication in vivo. J. Virol. 74:2046–2051.
30. **Kyono, K., M. Miyashiro, and I. Taguchi.** 2002. Human eukaryotic initiation factor 4AII associates with hepatitis C virus NS5B protein *in vitro*. Biochem. Biophys. Res. Commun. 292:659–666.
31. **Lee, W. C., D. Zabetakis, and T. Melese.** 1992. NSR1 is required for pre-rRNA processing and for the proper maintenance of steady-state levels of ribosomal subunits. Mol. Cell. Biol. 12:3865–3871.
32. **Lindenbach, B. D., M. J. Evans, A. J. Syder, B. Wolk, T. L. Tellinghuisen, C. C. Liu, T. Maruyama, R. O. Hynes, D. R. Burton, J. A. McKeating, and C. M. Rice.** 2005. Complete replication of hepatitis C virus in cell culture. Science 309:623–626.
33. **Lindenbach, B. D., and C. M. Rice.** 2005. Unravelling hepatitis C virus replication from genome to function. Nature 436:933–938.
34. **Lohmann, V., F. Korner, U. Herian, and R. Bartenschlager.** 1997. Biochemical properties of hepatitis C virus NS5B RNA-dependent RNA polymerase and identification of amino acid sequence motifs essential for enzymatic activity. J. Virol. 71:8416–8428.
35. **Lohmann, V., F. Korner, J. Koch, U. Herian, L. Theilmann, and R. Bartenschlager.** 1999. Replication of subgenomic hepatitis C virus RNAs in a hepatoma cell line. Science 285:110–113.
36. **Ma, Y., T. Shimakami, H. Luo, N. Hayashi, and S. Murakami.** 2004. Mutational analysis of hepatitis C virus NS5B in the subgenomic replicon cell culture. J. Biol. Chem. 279:25474–25482.
37. **Matthews, D. A.** 2001. Adenovirus protein V induces redistribution of nucleolin and B23 from nucleolus to cytoplasm. J. Virol. 75:1031–1038.
38. **McBride, A. E., A. Schlegel, and K. Kirkegaard.** 1996. Human protein Sam68 relocalization and interaction with poliovirus RNA polymerase in infected cells. Proc. Natl. Acad. Sci. USA 93:2296–2301.
39. **Mottola, G., G. Cardinali, A. Ceccacci, C. Trozzi, L. Bartholomew, M. R. Torrisi, E. Pedrazzini, S. Bonatti, and G. Migliaccio.** 2002. Hepatitis C virus

nonstructural proteins are localized in a modified endoplasmic reticulum of cells expressing viral subgenomic replicons. Virology 293:31–43.
40. Murata, T., T. Ohshima, M. Yamaji, M. Hosaka, Y. Miyanari, M. Hijikata, and K. Shimotohno. 2005. Suppression of hepatitis C virus replicon by TGF-beta. Virology 331:407–417.
41. Nisole, S., B. Krust, C. Callebaut, G. Guichard, S. Muller, J. P. Briand, and A. G. Hovanessian. 1999. The anti-HIV pseudopeptide HB-19 forms a complex with the cell-surface-expressed nucleolin independent of heparan sulfate proteoglycans. J. Biol. Chem. 274:27875–27884.
42. Nisole, S., B. Krust, E. Dam, A. Bianco, N. Seddiki, S. Loaec, C. Callebaut, G. Guichard, S. Muller, J. P. Briand, and A. G. Hovanessian. 2000. The HB-19 pseudopeptide 5[Kpsi(CH2N)PR]-TASP inhibits attachment of T lymphocyte- and macrophage-tropic HIV to permissive cells. AIDS Res. Hum. Retrovir. 16:237–249.
43. Nisole, S., B. Krust, and A. G. Hovanessian. 2002. Anchorage of HIV on permissive cells leads to coaggregation of viral particles with surface nucleolin at membrane raft microdomains. Exp. Cell Res. 276:155–173.
44. Nisole, S., E. A. Said, C. Mische, M. C. Prevost, B. Krust, P. Bouvet, A. Bianco, J. P. Briand, and A. G. Hovanessian. 2002. The anti-HIV pentameric pseudopeptide HB-19 binds the C-terminal end of nucleolin and prevents anchorage of virus particles in the plasma membrane of target cells. J. Biol. Chem. 277:20877–20886.
45. Osman, T. A., and K. W. Buck. 1997. The tobacco mosaic virus RNA polymerase complex contains a plant protein related to the RNA-binding subunit of yeast eIF-3. J. Virol. 71:6075–6082.
46. Piccininni, S., A. Varaklioti, M. Nardelli, B. Dave, K. D. Raney, and J. E. McCarthy. 2002. Modulation of the hepatitis C virus RNA-dependent RNA polymerase activity by the non-structural (NS) 3 helicase and the NS4B membrane protein. J. Biol. Chem. 277:45670–45679.
47. Pietschmann, T., V. Lohmann, G. Rutter, K. Kurpanek, and R. Bartenschlager. 2001. Characterization of cell lines carrying self-replicating hepatitis C virus RNAs. J. Virol. 75:1252–1264.
48. Qin, W., H. Luo, T. Nomura, N. Hayashi, T. Yamashita, and S. Murakami. 2002. Oligomeric interaction of hepatitis C virus NS5B is critical for catalytic activity of RNA-dependent RNA polymerase. J. Biol. Chem. 277:2132–2137.
49. Qin, W., T. Yamashita, Y. Shirota, Y. Lin, W. Wei, and S. Murakami. 2001. Mutational analysis of the structure and functions of hepatitis C virus RNA-dependent RNA polymerase. Hepatology 33:728–737.
50. Quadt, R., C. C. Kao, K. S. Browning, R. P. Hershberger, and P. Ahlquist. 1993. Characterization of a host protein associated with brome mosaic virus RNA-dependent RNA polymerase. Proc. Natl. Acad. Sci. USA 90:1498–1502.
51. Randall, G., A. Grakoui, and C. M. Rice. 2003. Clearance of replicating hepatitis C virus replicon RNAs in cell culture by small interfering RNAs. Proc. Natl. Acad. Sci. USA 100:235–240.
52. Said, E. A., B. Krust, S. Nisole, J. Svab, J. P. Briand, and A. G. Hovanessian. 2002. The anti-HIV cytokine midkine binds the cell surface-expressed nucleolin as a low affinity receptor. J. Biol. Chem. 277:37492–37502.
53. Saito, I., T. Miyamura, A. Ohbayashi, H. Harada, T. Katayama, S. Kikuchi, Y. Watanabe, S. Koi, M. Onji, Y. Ohta, et al. 1990. Hepatitis C virus infection is associated with the development of hepatocellular carcinoma. Proc. Natl. Acad. Sci. USA 87:6547–6549.
54. Seeff, L. B. 1997. Natural history of hepatitis C. Hepatology 26:21S–28S.
55. Semenkovich, C. F., R. E. Ostlund, Jr., M. O. Olson, and J. W. Yang. 1990. A protein partially expressed on the surface of HepG2 cells that binds lipoproteins specifically is nucleolin. Biochemistry 29:9708–9713.
56. Shimakami, T., M. Hijikata, H. Luo, Y. Y. Ma, S. Kaneko, K. Shimotohno, and S. Murakami. 2004. Effect of interaction between hepatitis C virus NS5A and NS5B on hepatitis C virus RNA replication with the hepatitis C virus replicon. J. Virol. 78:2738–2748.
57. Shirota, Y., H. Luo, W. Qin, S. Kaneko, T. Yamashita, K. Kobayashi, and S. Murakami. 2002. Hepatitis C virus (HCV) NS5A binds RNA-dependent RNA polymerase (RdRP) NS5B and modulates RNA-dependent RNA polymerase activity. J. Biol. Chem. 277:11149–11155.
58. Sinclair, J. F., and A. D. O'Brien. 2002. Cell surface-localized nucleolin is a eukaryotic receptor for the adhesin intimin-gamma of enterohemorrhagic Escherichia coli O157:H7. J. Biol. Chem. 277:2876–2885.
59. Srivastava, M., and H. B. Pollard. 1999. Molecular dissection of nucleolin's role in growth and cell proliferation: new insights. FASEB J. 13:1911–1922.
60. Take, M., J. Tsutsui, H. Obama, M. Ozawa, T. Nakayama, I. Maruyama, T. Arima, and T. Muramatsu. 1994. Identification of nucleolin as a binding protein for midkine (MK) and heparin-binding growth associated molecule (HB-GAM). J. Biochem. (Tokyo) 116:1063–1068.
61. Tsukiyama-Kohara, K., N. Iizuka, M. Kohara, and A. Nomoto. 1992. Internal ribosome entry site within hepatitis C virus RNA. J. Virol. 66:1476–1483.
62. Tu, H., L. Gao, S. T. Shi, D. R. Taylor, T. Yang, A. K. Mircheff, Y. Wen, A. E. Gorbalenya, S. B. Hwang, and M. M. Lai. 1999. Hepatitis C virus RNA polymerase and NS5A complex with a SNARE-like protein. Virology 263: 30–41.
63. Wakita, T., T. Pietschmann, T. Kato, T. Date, M. Miyamoto, Z. Zhao, K. Murthy, A. Habermann, H. G. Krausslich, M. Mizokami, R. Bartenschlager, and T. J. Liang. 2005. Production of infectious hepatitis C virus in tissue culture from a cloned viral genome. Nat. Med. 11:791–796.
64. Wang, C., P. Sarnow, and A. Siddiqui. 1993. Translation of human hepatitis C virus RNA in cultured cells is mediated by an internal ribosome-binding mechanism. J. Virol. 67:3338–3344.
65. Wang, Q. M., M. A. Hockman, K. Staschke, R. B. Johnson, K. A. Case, J. Lu, S. Parsons, F. Zhang, R. Rathnachalam, K. Kirkegaard, and J. M. Colacino. 2002. Oligomerization and cooperative RNA synthesis activity of hepatitis C virus RNA-dependent RNA polymerase. J. Virol. 76:3865–3872.
66. Weiner, A. J., M. J. Brauer, J. Rosenblatt, K. H. Richman, J. Tung, K. Crawford, F. Bonino, G. Saracco, Q. L. Choo, M. Houghton, et al. 1991. Variable and hypervariable domains are found in the regions of HCV corresponding to the flavivirus envelope and NS1 proteins and the pestivirus envelope glycoproteins. Virology 180:842–848.
67. Weiner, A. J., H. M. Geysen, C. Christopherson, J. E. Hall, T. J. Mason, G. Saracco, F. Bonino, K. Crawford, C. D. Marion, K. A. Crawford, et al. 1992. Evidence for immune selection of hepatitis C virus (HCV) putative envelope glycoprotein variants: potential role in chronic HCV infections. Proc. Natl. Acad. Sci. USA 89:3468–3472.
68. Yamashita, T., S. Kaneko, Y. Shirota, W. Qin, T. Nomura, K. Kobayashi, and S. Murakami. 1998. RNA-dependent RNA polymerase activity of the soluble recombinant hepatitis C virus NS5B protein truncated at the C-terminal region. J. Biol. Chem. 273:15479–15486.
69. Yanagi, M., M. St. Claire, S. U. Emerson, R. H. Purcell, and J. Bukh. 1999. *In vivo* analysis of the 3′ untranslated region of the hepatitis C virus after *in vitro* mutagenesis of an infectious cDNA clone. Proc. Natl. Acad. Sci. USA 96:2291–2295.
70. Yang, T. H., W. H. Tsai, Y. M. Lee, H. Y. Lei, M. Y. Lai, D. S. Chen, N. H. Yeh, and S. C. Lee. 1994. Purification and characterization of nucleolin and its identification as a transcription repressor. Mol. Cell. Biol. 14:6068–6074.
71. Yi, M., and S. M. Lemon. 2003. 3′ nontranslated RNA signals required for replication of hepatitis C virus RNA. J. Virol. 77:3557–3568.
72. Zhong, J., P. Gastaminza, G. Cheng, S. Kapadia, T. Kato, D. R. Burton, S. F. Wieland, S. L. Uprichard, T. Wakita, and F. V. Chisari. 2005. Robust hepatitis C virus infection *in vitro*. Proc. Natl. Acad. Sci. USA 102:9294–9299.

Journal of General Virology (2007), 88, 432–440 DOI 10.1099/vir.0.82319-0

Dual effect of APOBEC3G on *Hepatitis B virus*

Chiemi Noguchi,[1,2] Nobuhiko Hiraga,[1,2] Nami Mori,[1,2] Masataka Tsuge,[1,2] Michio Imamura,[1,2] Shoichi Takahashi,[1,2] Yoshifumi Fujimoto,[2,3] Hidenori Ochi,[2,3] Hiromi Abe,[1,3] Toshiro Maekawa,[3] Hiromi Yatsuji,[1,4] Kotaro Shirakawa,[5] Akifumi Takaori-Kondo[5] and Kazuaki Chayama[1,2,3]

Correspondence
Kazuaki Chayama
chayama@hiroshima-u.ac.jp

[1]Department of Medicine and Molecular Science, Division of Frontier Medical Science, Programs for Biomedical Research, Graduate School of Biomedical Sciences, Hiroshima University, 1-2-3 Kasumi, Minami-ku, Hiroshima-shi 734-8551, Japan

[2]Liver Research Project Center, Hiroshima University, Hiroshima, Japan

[3]Laboratory for Liver Diseases, SNP Research Center, The Institute of Physical and Chemical Research (RIKEN), Yokohama 230-0045, Japan

[4]Department of Gastroenterology, Toranomon Hospital, Tokyo, Japan

[5]Department of Hematology and Oncology, Graduate School of Medicine, Kyoto University, Kyoto 606-8507, Japan

G to A hypermutation of *Hepatitis B virus* (HBV) and retroviruses appears as a result of deamination activities of host APOBEC proteins and is thought to play a role in innate antiviral immunity. Alpha and gamma interferons (IFN-α and -γ) have been reported to upregulate the transcription of APOBEC3G, which is known to reduce the replication of HBV. We investigated the number of hypermutated genomes under various conditions by developing a quantitative measurement. The level of hypermutated HBV in a HepG2 cell line, which is semi-permissive for retrovirus, was 2.3 in 10^4 HBV genomes, but only 0.5 in 10^4 in permissive Huh7 cells. The level of APOBEC3G mRNA was about ten times greater in HepG2 cells than in Huh7 cells. Treatment of HepG2 cells with either IFN-α or -γ increased the transcription of APOBEC3G and hypermutation of HBV. These mRNAs and hypermutation of HBV genomes were induced more prominently by IFN-γ than by IFN-α. Both IFNs decreased the number of replicative intermediate of HBV. Overexpression of APOBEC3G reduced the number of replicative intermediate of HBV and increased hypermutated genomes 334 times, reaching 968 in 10^4 genomes. Deamination-inactive APOBEC3G did not induce hypermutation, but reduced the virus equally. Our results suggest that APOBEC3G, upregulated by IFNs, has a dual effect on HBV: induction of hypermutation and reduction of virus synthesis. The effect of hypermutation on infectivity should be investigated further.

Received 22 June 2006
Accepted 10 October 2006

INTRODUCTION

Hepatitis B virus (HBV) is a small, enveloped DNA virus with partially double-stranded DNA as a genome (Ganem & Schneider, 2001; Seeger & Mason, 2000). The virus replicates through transcription of pregenome RNA and reverse transcription, like retroviruses (Skalka & Goff, 1993; Summers & Mason, 1982). Infection with HBV causes chronic hepatitis and often leads to liver cirrhosis and hepatocellular carcinoma (Wright & Lau, 1993; Bruix & Llovet, 2003; Ganem & Prince, 2004).

Recent reports have shown that a cytidine deaminase, APOBEC3G, which is packaged in human immunodeficiency virus (HIV) virions in non-permissive cells, induces G to A hypermutation to a nascent reverse transcript of HIV and serves as part of the innate antiviral activity (Mangeat *et al.*, 2003; Zhang *et al.*, 2003; Lecossier *et al.*, 2003; Harris *et al.*, 2003). Recent studies have demonstrated that a small number of HBV DNA in serum samples of patients with chronic HBV infection contains hypermutated genomes (Gunther *et al.*, 1997; Suspene *et al.*, 2005a; Noguchi *et al.*, 2005). We reported previously that there are small numbers of hypermutated genomes in serum samples of the majority of patients with chronic HBV infection and that G to A hypermutation could be induced in cultured liver cells derived from HepG2 cell lines (Noguchi *et al.*, 2005) using a peptide nucleic acid-mediated PCR clamping method. Suspene *et al.* (2005a) developed the more sensitive differential DNA denaturation (3D)-PCR method to detect hypermutated genomes and found that some APOBEC proteins induce G to A, and in some cases C to T, hypermutations in HBV DNA (Suspene *et al.*, 2005a). Why only a very small proportion of the HBV genome is hypermutated is unknown at present. Furthermore, the

mechanism that controls the level of APOBEC protein expression and degree of hypermutation has not been fully investigated. Recently, Tanaka *et al.* (2006) identified an interferon (IFN)-stimulated response element (ISRE) in the promoter region of APOBEC3G and showed that IFN-α upregulates transcription of APOBEC3G. Peng *et al.* (2006) also reported that IFN-α and -γ upregulate mRNA transcription of APOBEC proteins. However, these reports did not analyse whether increased numbers of APOBEC proteins actually increase hypermutation. More recently, Bonvin *et al.* (2006) demonstrated that IFN induces transcription of APOBEC proteins and increases hypermutation of HBV.

IFNs are cytokines that play a major role against many pathogens (Samuel, 2001; Colonna *et al.*, 2002; Grandvaux *et al.*, 2002). We also reported in a previous study that both IFN-α and -γ reduce virus replication in stably HBV-transfected cell lines without inducing a remarkable increase in G to A hypermutation (Noguchi *et al.*, 2005). However, the method used in previous experiments for detection of hypermutation was not as sensitive as the method of Suspene *et al.* (2005a, b) and not quantitative. To assess the level of hypermutation, a reliable measurement of hypermutated genome is needed. In the present study, we developed a new and sensitive method for the measurement of hypermutated genome levels. Using this method, we show here that both IFN-α and -γ increased the levels of hypermutated genomes in cultured cell lines. Furthermore, both IFNs increased the mRNA level of APOBEC3G. We also performed overexpression experiments to examine whether APOBEC3G and its inactive mutants increase the levels of hypermutation and reduce HBV replication.

METHODS

Plasmid constructs. The expression vector for haemagglutinin (HA)-tagged human APOBEC3G, pcDNA3/HA-A3G, was constructed as described previously (Kobayashi *et al.*, 2004). APOBEC3F cDNA was obtained by modifying APOBEC3F like (IMAGE clones from Open Biosystems) to have the same sequence as human APOBEC3F transcript variant 1 (GenBank NM_145298) and cloned into pcDNA3/HA (Invitrogen). APOBEC3G mutants were constructed using a QuikChange mutagenesis kit (Stratagene). The construction of wild-type HBV 1.4 genome length, pTRE-HB-wt, has been described previously (GenBank accession no. AB206816) (Tsuge *et al.*, 2005).

Cell culture and transfection. Huh7 and HepG2 cell lines were grown in Dulbecco's modified Eagle's medium supplemented with 10 % (v/v) fetal calf serum at 37 °C in 5 % CO_2. Cells were seeded to semi-confluence in six-well tissue culture plates. Transient transfection of the plasmids into HepG2 and Huh7 cell lines was performed using *Trans*IT-LT1 (Mirus) according to the instructions provided by the supplier. A plasmid encoding a secreted form of human placental alkaline phosphatase (SEAP) was co-transfected to adjust the transfection efficiency. The SEAP assay in the culture medium was performed using the Great EscAPe SEAP Reporter System 3 (BD Bioscience).

T23 cells are HepG2 cells stably transfected with the plasmid pTRE-HB-wt. They were cultured using a method described previously (Tsuge *et al.*, 2005). Cells were seeded to semi-confluence in six-well tissue culture plates and then treated with medium containing either IFN-α (Hayashibara Biochemical Laboratories) or IFN-γ (Shionogi & Co.). The cells were harvested 12–72 h after IFN treatment. Core-associated HBV DNA was extracted from the cells for HBV DNA quantification and quantitative analysis of G to A hypermutated genomes (Noguchi *et al.*, 2005).

Analysis of core-associated HBV DNA. The cells were harvested 4 days after transfection and lysed with 250 µl lysis buffer [10 mM Tris/HCl pH 7.4, 140 mM NaCl and 0.5 % (v/v) NP-40] followed by centrifugation for 2 min at 15 000 *g*. The core-associated HBV genome was immunoprecipitated from the supernatant by mouse anti-core monoclonal antibody anti-HBc determinant α (Institute of Immunology, Tokyo, Japan) and subjected to quantitative analysis after SDS/proteinase K digestion followed by phenol extraction and ethanol precipitation. Quantitative analysis was performed by real-time PCR using the 7300 Real-Time PCR system (Applied Biosystems). The primers used for amplification were #1, 5′-ACTTCAACCCCAACAMRRATCA-3′ (nt 2978–2999) [numbers are those of HBV subtype C reported by Norder *et al.* (1994)] and #2, 5′-AGAGYTTGKTGGAATGTKGTGGA-3′ (nt 24–1), where M is A/C, R is G/A, Y is T/C and K is G/T. The probe was a 6-carboxyfluorescein (FAM)-labelled minor-groove binder (MGB) probe, 5′-(FAM)-TTAGAGGTGGAGAGATGG-(MGB)-3′ (nt 3184–3167). Real-time PCRs were set up in 25 µl TaqMan Universal Master Mix with 1 µl DNA solution, 0.9 µM each primer and 0.25 µM probe. The amplification conditions were 2 min at 50 °C, 10 min at 95 °C, followed by 40 cycles of amplification (denaturation at 95 °C for 15 s, annealing at 55 °C for 30 s and extension at 62 °C for 90 s).

Amplification and analysis of hypermutated HBV genomes by 3D-PCR. HBV DNA was extracted from 100 µl serum obtained from a chronic HBV carrier (genotype C) by SMITEST (MBL International) and was dissolved in 20 µl H_2O. Hypermutated genomes were detected by modified 3D-PCR using primers #1 and #2 and DNA solution from serum containing 8.0×10^7 or 2.3×10^5 copies of core-associated HBV DNA in 25 µl of 100 mM Tris/HCl pH 8.3, 50 mM KCl, 15 mM $MgCl_2$, 0.2 mM each dNTP, 10 pmol each primer and 1.25 U *Taq* DNA polymerase (Gene Taq, Nippon Gene Co.), together with 0.25 µg anti-*Taq* high (TOYOBO Co.). The amplification conditions included an initial denaturation step at 83–95 °C for 5 min, followed by 45 cycles of denaturation at 83–95 °C for 1 min, annealing at 50 °C for 30 s, extension at 72 °C for 30 s followed by 10 min of final extension. Amplicons were separated by electrophoresis on 2 % (w/v) agarose gel, cloned and sequenced in an ABI PRISM 3130 Genetic Analyzer with a BigDye Terminator version 3.1 cycle sequencing ready reaction kit (Applied Biosystems). The PCR products were also analysed on Hanse Analytik (HA)-yellow gel as described previously (Suspene *et al.*, 2005b; Tsuge *et al.*, 2005; Abu-Daya *et al.*, 1995).

Quantitative analysis of hypermutated genomes by real-time PCR. Hypermutated genomes were quantified by real-time PCR using the 7300 Real-Time PCR system (Applied Biosystems) and the above primers and probes. The amplification conditions included activation at 95 °C for 10 min followed by initial denaturation at 88 °C for 20 min and 45 cycles of amplification (denaturation at 88 °C for 15 s, annealing at 50 °C for 30 s and extension at 62 °C for 90 s). We chose 88 °C as this temperature is appropriate for detection of about 20 % hypermutated genomes. There are 200–300 such hypermutated genomes in 10^4 genomes present in HepG2 cells transiently transfected with APOBEC3G. The buffer comprised 10 mM Tris/HCl pH 8.3, 50 mM KCl, 3 mM $MgCl_2$, 10 mM EDTA, 60 nM Passive Reference 1 (Applied Biosystems), 0.2 mM each dNTP, 0.9 µM each primer, 0.25 µM probe, 5×10^6 copies of HBV DNA

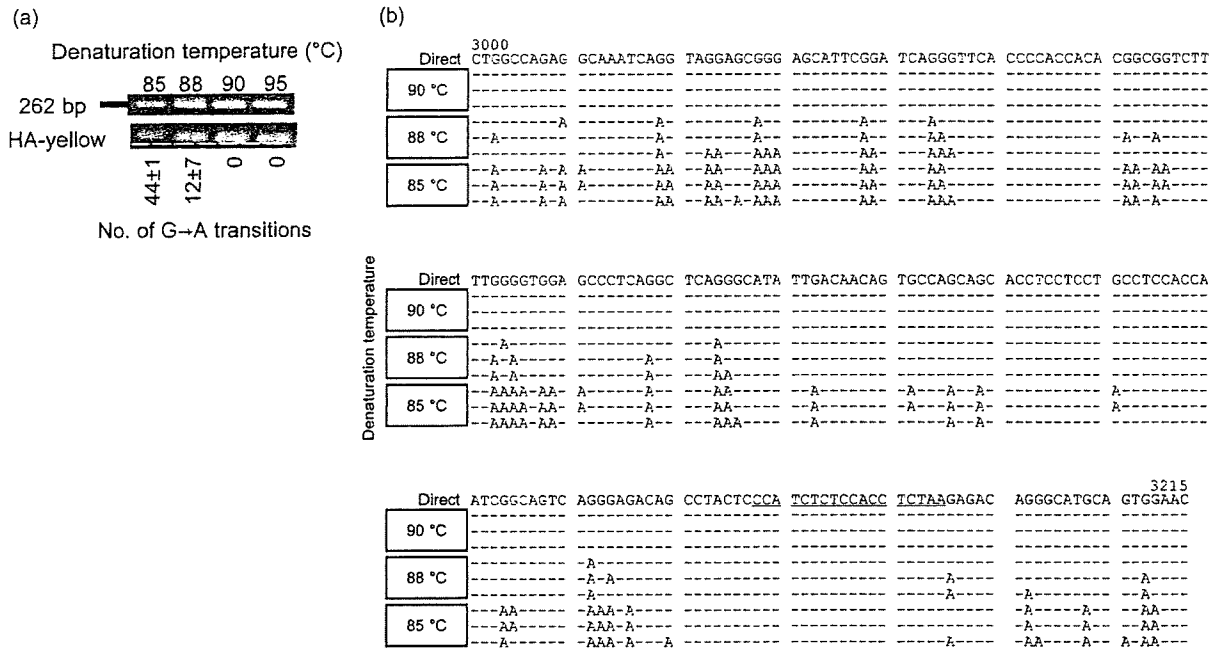

Fig. 1. Amplification of HBV DNA by 3D-PCR. (a) Detection of hypermutated genomes by HA-yellow agarose gel electrophoresis. The numbers of G to A transitions are expressed as means ± SD generated from the sequence analysis of five independent clones from PCR products. The white dotted line was added to help visualize the retardation of AT-rich DNA in HA-yellow agarose gel. (b) Nucleotide sequences of HBV amplified by 3D-PCR. The nucleotide sequences obtained by direct sequencing are used as a reference sequence. The nucleotide sequences where the probe hybridizes are underlined. Note that the number of G to A mutations correlates with denaturation temperature.

and 0.625 U AmpliTaq Gold DNA polymerase (Applied Biosystems) in a final volume of 25 µl. A standard curve was constructed by the simultaneous amplification of serial dilutions of the 3D-PCR products.

Western blot analysis. Cell lysates were prepared as described above, resolved on 10% (w/v) SDS-polyacrylamide gels and transferred to nitrocellulose membranes (Whatman) via electro-blotting. The membranes were incubated with anti-haemagglutinin fusion epitope monoclonal antibody (Roche) or with anti-β-actin monoclonal antibody (Sigma-Aldrich) followed by incubation with horseradish peroxidase-conjugated donkey anti-rabbit antibody or sheep anti-mouse immunoglobulin (Amersham Biosciences). Proteins were visualized via the ECL system (Amersham Biosciences).

Quantification of mRNA of APOBEC3G or APOBEC3F by reverse transcription and real-time PCR. Total RNA was extracted from HepG2 cell lines by using an RNeasy Mini kit (Qiagen). The RNA was reverse transcribed with random primers and Moloney murine leukemia virus reverse transcriptase (ReverTra Ace, TOYOBO Co.) at 42 °C for 60 min according to the instructions provided by the manufacturer. Quantitative analysis of APOBEC3G and APOBEC3F cDNA was performed by real-time PCR using TaqMan Gene Expression assays (Applied Biosystems). To confirm that the APOBEC3G and -3F PCR primers specifically amplify the target genes, quantitative PCR on the expression plasmids encoding human APOBEC3G and -3F, used as templates, was performed. No cross amplification was observed, even when we used 10^7 copies of APOBEC3G plasmid in the amplification reaction of APOBEC3F and vice versa. A standard curve was constructed by the amplification of serial dilutions of the known number of plasmids containing human APOBEC3G and APOBEC3F. The target cDNA was normalized to the endogenous RNA level of the housekeeping reference gene glyceraldehyde-3-phosphate dehydrogenase (GAPDH). The primers and FAM-labelled probe used to quantify GAPDH were purchased from Applied Biosystems.

Infectivity of luciferase reporter viruses produced from HepG2 and Huh7 cell lines. Luciferase reporter viruses with or without viral infectivity factor (Vif) were prepared by co-transfection of pNL43/ΔEnv-Luc (wild-type) or pNL43/ΔEnvΔvif-Luc (ΔVif) plus pVSV-G together with a mock vector or expression vectors for A3G by Lipofectamine (Invitrogen) as described previously (Janini *et al.*, 2001; Shindo *et al.*, 2003). Productive infection was measured by luciferase activity. Values were presented as percentage of infectivity relative to the value of each virus without expression of APOBEC3G proteins.

RESULTS

Quantitative analysis of hypermutated genome by real-time PCR

Using serum samples from a patient with a high viral load, we amplified a large number of hypermutated genomes by 3D-PCR and detected them by HA-yellow agarose gel electrophoresis (Fig. 1a). Nucleotide sequence analysis

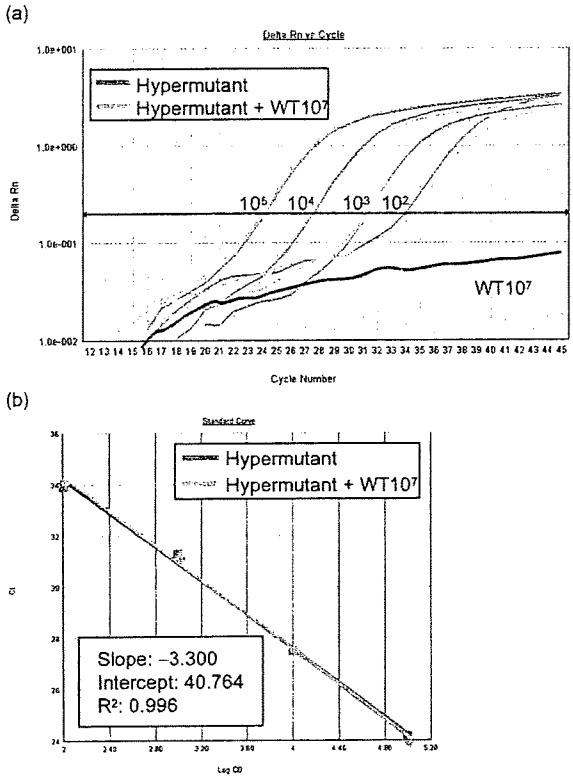

Fig. 2. Quantitative measurement of hypermutated HBV DNA using 3D-PCR combined with real-time PCR. The indicated numbers (10^2–10^5) of hypermutated genomes alone (orange lines) and a mixture of wild-type plus hypermutated genomes (green lines) were amplified by 3D-PCR. 3D-PCR did not result in amplification of wild-type sequence (purple line). Denaturation temperature was 88 °C.

showed detection of more heavily hypermutated genomes at lower denaturation temperatures (Fig. 1b). To develop quantitative measurement, we selected sequences with many G residues, designed primers that contained only a small number of G residues and used degenerate primers. A probe sequence was designed without a G residue. Using this primer and probe set, we could amplify only hypermutated genomes (Fig. 2). When hypermutated and non-mutated genomes were co-amplified, only hypermutated genomes were successfully amplified using the above primer and probe set (Fig. 2b). Non-hypermutated genomes (10^7 copies) were not amplified, although conventional PCR amplified both mutated and non-mutated genomes equally (data not shown). We also tried to detect only slightly (four of the 58 G residues) mutated genomes by 3D-PCR, but could not detect such genomes. It should thus be noted that the quantitative measurement we developed in this study detects only hypermutated genomes.

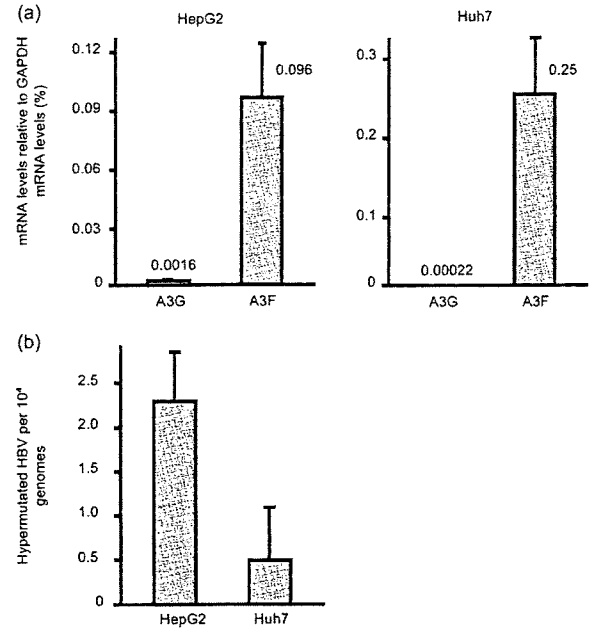

Fig. 3. Expression levels of APOBEC3G and -3F protein mRNAs in HepG2 and Huh7 cell lines. (a) mRNAs were extracted from cultured cell lines and the number of mRNA was quantified by real-time PCR with a probe for APOBEC3G and -3F. The expression levels were expressed as a percentage of GAPDH mRNA. (b) Number of hypermutated HBV genomes measured by real-time 3D-PCR in HepG2 and Huh7 cell lines transiently transfected with pTRE-HBV-wt. Results are means ± SD values of three independent experiments.

Detection of APOBEC3G mRNA and hypermutated genomes in semi-permissive and permissive cell lines

In retrovirus studies, it is known that some cell lines allow production of infectious retrovirus virions with Vif deficiency (permissive cells) while others do not. The difference between semi-permissive and permissive cell lines is the expression of APOBEC3G (Mangeat *et al.*, 2003; Zhang *et al.*, 2003; Lecossier *et al.*, 2003; Harris *et al.*, 2003; Shirakawa *et al.*, 2006). Thus, we examined the expression of APOBEC3G in both HepG2 and Huh7 cell lines. The APOBEC3G mRNA level detected by real-time PCR was very low (approx. 0.002 % relative to GAPDH mRNA) and about ten times greater in HepG2 cells than in Huh7 cells (Fig. 3a).

The number of hypermutated genomes in HepG2 cells transiently transfected with pTRE-HB-wt was about five times that in Huh7 cells (Fig. 3b). Vif-deficient HIV-1 virions produced from HepG2 cell exhibited very low infectivity compared with wild-type (Fig. 4a). In contrast, the infectivity of HIV-1 virions produced by Huh7 was

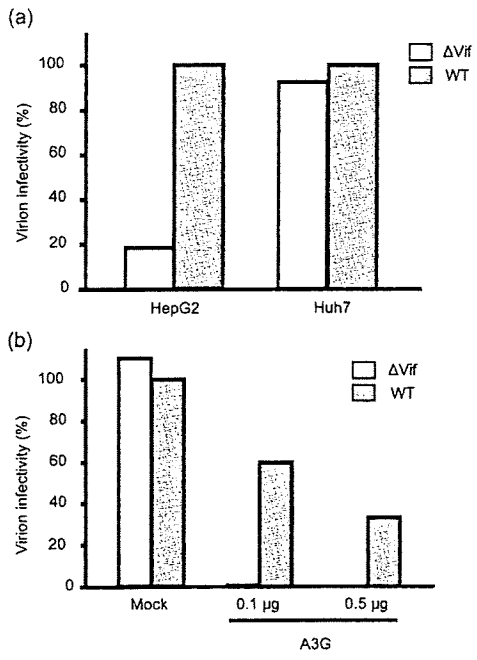

Fig. 4. Infectivity of HIV-1 virions produced from HepG2 and Huh7 cell lines. (a) Wild-type and mutant viruses lacking Vif protein produced from the two cell lines were examined for infectivity as described in Methods. The relative infectivity of the wild-type is shown. (b) Effect of APOBEC3G (A3G) expression on infectivity. HIV-1 virions produced by Huh7 cells co-transfected with the indicated number of APOBEC3G expression plasmid were used for measurement of infectivity.

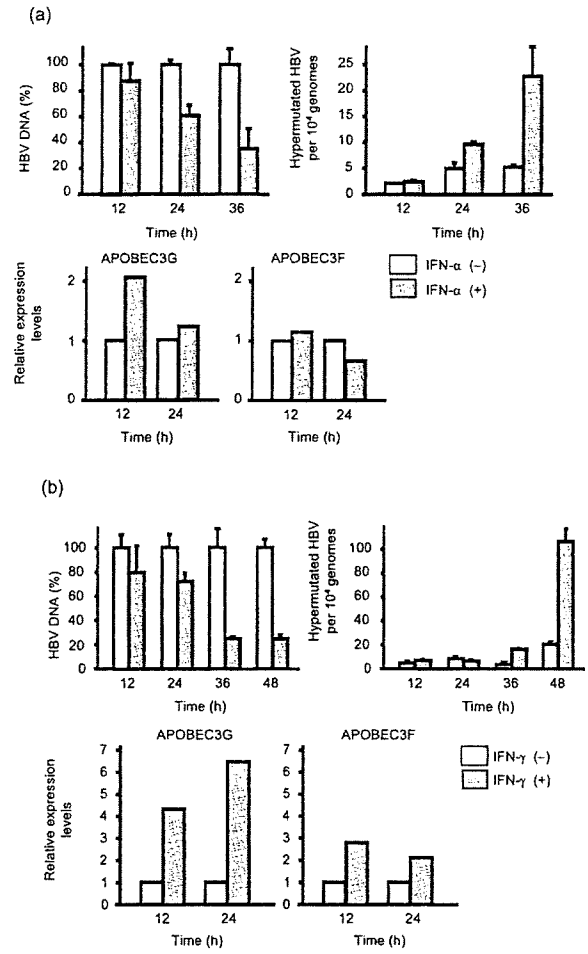

Fig. 5. Effects of IFN-α and -γ on HBV-producing cells. (a) The IFN-α-treated and -untreated HBV-producing T23 cell line was harvested at the indicated time after IFN treatment and examined for the number of core-associated HBV DNA, the number of hypermutated genome and mRNAs of APOBEC3G and APOBEC3F. (b) IFN-γ-treated and -untreated HBV-producing T23 cell line was examined as described in (a). Results are means ± SD values of three independent experiments.

similar to that of the wild-type virus (Fig. 4a). Transient expression experiments showed that the expression of APOBEC3G in Huh7 cell lines reduced infectivity of wild-type HIV-1 produced in these cell lines in a dose-dependent manner (Fig. 4b). Infectivity of Vif-deficient HIV-1 was reduced to almost undetectable levels (Fig. 4b). Thus, APOBEC3G effectively suppressed the production of infectious HIV in these cell lines.

Both IFN-α and -γ induce APOBEC3G mRNA expression and hypermutation of HBV genomes and reduce replication of HBV

We treated HepG2 cell lines stably transfected with 1.4 genome length construct HBV (Tsuge *et al.*, 2005) with either IFN-α or -γ to examine their influence on the expression of APOBEC3G mRNA and G to A hypermutation of HBV genomes. Chronological studies showed that the core-associated HBV DNA in the stably HBV-producing cell line gradually decreased until 36 h after IFN-α treatment (Fig. 5a). Expression levels of APOBEC3G mRNA, but not those of APOBEC3F, increased in this cell line at 12 h after the IFN treatment (Fig. 5a). Hypermutated genomes in this cell line increased with time until 36 h after IFN-α treatment. Similarly, the core-associated HBV DNA decreased gradually to about 20 % of the levels in untreated cells after IFN-γ treatment (Fig. 5b). The increase in APOBEC3G mRNA expression was more prominent after IFN-γ than after IFN-α treatment. The level of APOBEC3F mRNA was also about double that of untreated cells. G to A hypermutation of HBV genomes increased markedly with time after IFN-γ treatment (Fig. 5b).

We further examined the effect of IFN on reduction of HBV replication and induction of hypermutation by comparing the effects of different doses of IFN-α and -γ. Both IFN-α

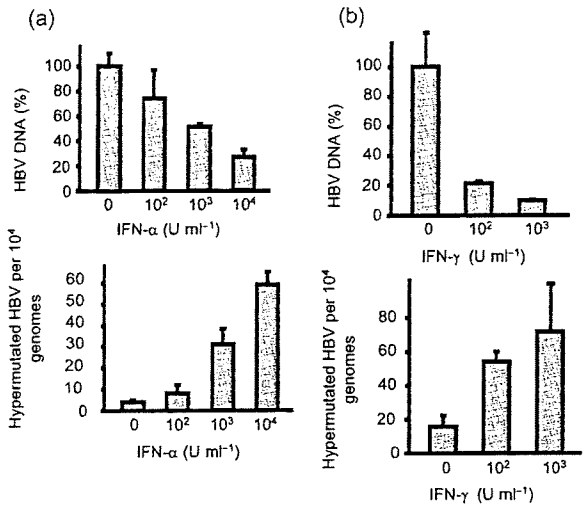

Fig. 6. Dose-dependent reduction of HBV replication and hypermutation of genomic sequences. HBV-producing cell line T23 was harvested after (a) IFN-α and (b) IFN-γ treatment for 72 h. The number of core-associated HBV DNA and the number of hypermutated genomes were measured. Results are means ± SD values of three independent experiments.

and -γ treatment decreased core-associated HBV DNA in a dose-dependent manner (Fig. 6). Hypermutation of HBV genomes also increased with higher doses of IFN (Fig. 6).

Expression of APOBEC3G increases hypermutation of the HBV genome

To confirm that the increase in hypermutation of the HBV genome is induced by the effect of APOBEC3G, we performed expression experiments of APOBEC3G and its deaminase function-deficient mutants into HepG2 cell lines and measured the number of hypermutated HBV genomes. Transient expression experiments showed that the number of HBV DNA was decreased by co-transfection of APOBEC3G in HepG2 cells (Fig. 7a). 3D-PCR and detection with HA-yellow agarose gel electrophoresis showed the presence of heavily hypermutated genomes (Fig. 7b). No amplification was observed at the 81 °C denaturation temperature (data not shown). Quantitative analysis showed an about 334-fold increase in hypermutated genomes compared with mock-transfected control cells (Fig. 7c). However, the proportion of hypermutated genomes was 9.68 % (968 in 10^4 genomes).

To confirm the effect of APOBEC3G on HBV hypermutation, we transfected wild-type and inactive mutants of APOBEC3G (Fig. 8a, b) into Huh7 cells. Wild-type APOBEC3G effectively induced hypermutation of HBV genomes and reduced the replication of HBV. In contrast, insufficient deaminase activity in the E67Q mutant induced less hypermutation of HBV genomes than in the wild-type. No increase in hypermutation was observed in cell lines transfected with deamination-defective E259Q and E67Q/E259Q mutants, although the number of HBV replication was reduced in these cells (Fig. 8a). We observed similar reduction in HBV replication by transient transfection of APOBEC3F. Induction of hypermutation by APOBEC3F was less efficient than by wild-type and the E67Q mutant of

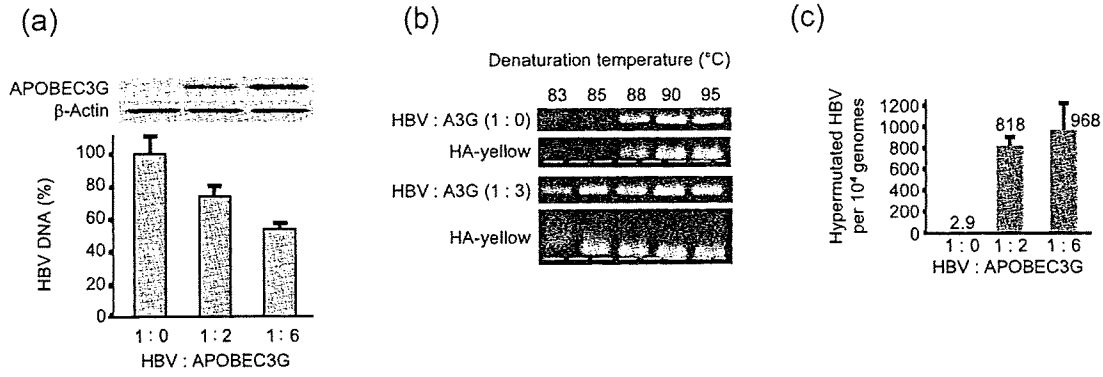

Fig. 7. Effects of APOBEC3G expression on HBV hypermutation. A plasmid containing 1.4 genome length HBV DNA was co-transfected with pcDNA3/HA-A3G into HepG2 cells. At 72 h after transfection, the cells were harvested. (a) Quantification of core-associated HBV DNA and Western blot analysis of cytoplasmic extracts with anti-HA or anti-β-actin antibody. (b) Detection of hypermutated genomes by HA-yellow agarose gel electrophoresis. Hypermutated genomes in the presence or absence of APOBEC3G-HA were amplified by 3D-PCR. The white dotted line was added to help visualize the retardation of AT-rich DNA in HA-yellow agarose gel. (c) Quantification analysis of hypermutated genomes by real-time 3D-PCR. Results are means ± SD values of three independent experiments.

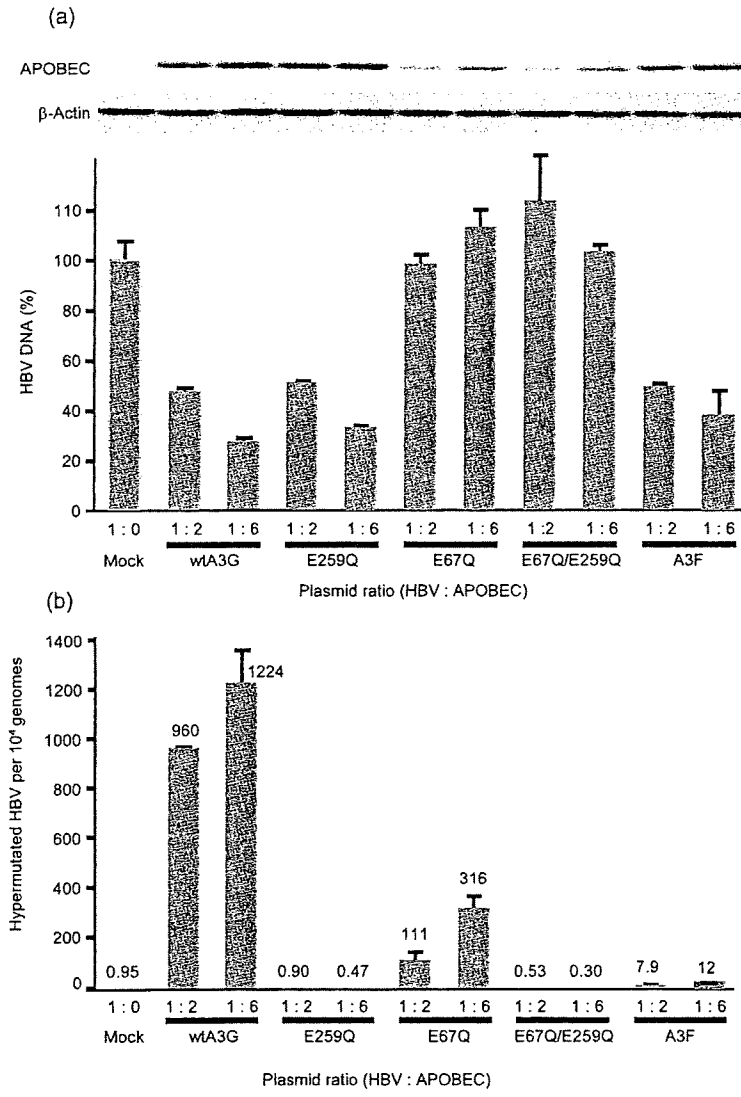

Fig. 8. Effect of APOBEC proteins on HBV hypermutation. A plasmid containing 1.4 genome length HBV DNA was co-transfected with wild-type, enzymically impaired APOBEC3G mutants (E67Q, E259Q, E67Q/E259Q) and APOBEC3F into Huh7 cells (plasmid ratio HBV : APOBEC = 1 : 2 or 1 : 6). The cells were harvested at 96 h after transfection. (a) Quantification of core-associated HBV DNA and Western blot analysis of cytoplasmic extracts with anti-HA or anti-β-actin antibody. (b) Quantification of hypermutated genomes by real-time 3D-PCR. Results are means ± SD values of three independent experiments.

APOBEC3G. These results suggest that hypermutation of HBV contributes very little to reduce the number of replicative intermediate.

DISCUSSION

Induction of G to A hypermutation in HIV has been reported as part of host innate immunity against virus infection (Mangeat *et al.*, 2003; Zhang *et al.*, 2003; Lecossier *et al.*, 2003; Harris *et al.*, 2003; Sheehy *et al.*, 2002). We and others have reported the presence of hypermutated genomes of HBV in serum samples of chronically infected patients and in HepG2 cell lines (Gunther *et al.*, 1997; Suspene *et al.*, 2005a; Noguchi *et al.*, 2005; Rosler *et al.*, 2004). Hypermutation of HBV was induced in hepatocytes (Noguchi *et al.*, 2005), and expression of APOBEC proteins in liver cell-derived cell lines increased hypermutation (Suspene *et al.*, 2005b; Rosler *et al.*, 2004). However, the estimated number of hypermutated genomes in chronically infected patients is very low (Noguchi *et al.*, 2005; Suspene *et al.*, 2005b). The reason for the partial hypermutation of HBV remains an enigma. It might be due to the low expression levels of APOBEC proteins in liver cells (Jarmuz *et al.*, 2002). Alternatively, rapid packaging of pregenome RNA into capsid might prevent access of APOBEC3G to the first strand DNA. Furthermore, rapid degradation of edited HBV genomes by uracil DNA glycosylase in liver cells might also explain the low number of hypermutated genomes.

The mechanism that controls the activities of APOBEC proteins to cause hypermutation has not been analysed until

recently. Tanaka *et al.* (2006) reported that IFN-α increases the expression levels of APOBEC3G mRNA. They reported the presence of ISRE elements in the promoter region of APOBEC3G and that the promoter was activated by IFN-α. However, they did not examine the occurrence of G to A hypermutation in their experiments. Moreover, Peng *et al.* (2006) showed that IFN-α and -γ cooperatively induce APOBEC3G expression and that the inhibition of HIV production by a small number of IFN is cancelled by a small interfering RNA (siRNA) against APOBEC3G. More recently, Bonvin *et al.* (2006) demonstrated that IFN-α induces transcription of APOBEC proteins. They showed that IFN treatment increased APOBEC3B, -3C, -3F and -3G mRNAs, particularly when they used primary cultured hepatocytes. They also reported that they were able to detect hypermutated genomes after transfection of APOBEC3 plasmids, but did not measure the direct effect of IFN on G to A hypermutation.

These studies did not analyse quantitatively the increase in hypermutation of viral genomes. The studies that analysed the expression of APOBEC protein and reduction of HBV DNA also did not analyse quantitatively the number of hypermutated genome (Suspene *et al.*, 2005a; Noguchi *et al.*, 2005; Turelli *et al.*, 2004a, b; Rosler *et al.*, 2005). In the present study, we developed a method that accurately measures the level of hypermutation using real-time PCR. It is often difficult to design a primer set and a probe to detect G to A hypermutation because they are located in a region with many G residues, but the primer and probe sequences should not contain any. It is thus possible that we did not see any C to T substitution because we did not design a primer–probe set to detect this substitution. We also tried to select such a primer–probe set applicable for all genotypes of HBV, but were able to select only one suitable for genotype C.

Using this method, we demonstrated that both IFN-α and -γ increased G to A hypermutation of the HBV genome. Although the expression levels of APOBEC3G increased after IFN treatment, we did not observe an apparent shift of preferred dinucleotide sequence of APOBEC proteins from 3F to 3G. This is probably because the increase in APOBEC3G is only slight (Fig. 5).

The exact mechanism by which IFNs activate the transcription of APOBEC3G is unknown. Furthermore, what kind of sensor(s) detects HBV infection and how the signal is communicated for the production of IFNs and subsequent induction of effector molecules have not been analysed yet. Although the importance of the IFN system in eliminating HBV and its possible mechanism have been reported (Wieland *et al.*, 2004a, b, 2005), further studies are needed to fully describe the mechanism of action of IFNs including the activation of APOBEC3G.

We also demonstrated that the number of hypermutated genomes increased with the expression of APOBEC3G and APOBEC3F (Fig. 8), but not in deaminase-inactive mutants, as demonstrated previously in HIV studies (Shindo *et al.*, 2003; Newman *et al.*, 2005). However, these mutants also reduced the replication of HBV almost to the wild-type level. This suggests that the contribution of hypermutation of HBV to the reduction of virus replication is only minimal and supports the previous report that showed that APOBEC3G reduced the replication of HBV through inhibition of packaging of the pregenome (Turelli *et al.*, 2004a). However, the effect of hypermutation on infectivity of the virus should be investigated further. The effects of APOBEC proteins, including other family members, especially under physiological conditions, should also be examined further. Whether any HBV protein inhibits deamination of the genomic DNA awaits further investigation. Furthermore, the mechanism that enables HBV to cause chronic infection, especially escape from innate antiviral immunity, should also be clarified in order to control chronic HBV infection and reduce HBV-related morbidity.

ACKNOWLEDGEMENTS

This work was carried out at the Research Center for Molecular Medicine, Faculty of Medicine, Hiroshima University. The authors thank Kana Kunihiro, Asako Kozono, Hiromi Ishino, Rie Akiyama, Eiko Miyoshi and Kiyomi Toyota for the excellent technical assistance, and Yoshiko Nakata for the secretarial assistance. This work was supported in part by a Grant-in-Aid for Scientific Research and development from the Ministry of Education, Sports, Culture and Technology and the Ministry of Health, Labour and Welfare.

REFERENCES

Abu-Daya, A., Brown, P. M. & Fox, K. R. (1995). DNA sequence preferences of several AT-selective minor groove binding ligands. *Nucleic Acids Res* **23**, 3385–3392.

Bonvin, M., Achermann, F., Greeve, I., Stroka, D., Keogh, A., Inderbitzin, D., Candinas, D., Sommer, P., Wain-Hobson, S. & other authors (2006). Interferon-inducible expression of APOBEC3 editing enzymes in human hepatocytes and inhibition of hepatitis B virus replication. *Hepatology* **43**, 1364–1374.

Bruix, J. & Llovet, J. M. (2003). Hepatitis B virus and hepatocellular carcinoma. *J Hepatol* **39** (Suppl. 1), S59–S63.

Colonna, M., Krug, A. & Cella, M. (2002). Interferon-producing cells: on the front line in immune responses against pathogens. *Curr Opin Immunol* **14**, 373–379.

Ganem, D. & Schneider, R. (2001). *Hepadnaviridae*: the viruses and their replication. In *Fields Virology*, 4th edn, pp. 2923–2969. Edited by D. M. Knipe & P. M. Howley. Baltimore: Lippincott Williams & Wilkins.

Ganem, D. & Prince, A. M. (2004). Hepatitis B virus infection - natural history and clinical consequences. *N Engl J Med* **350**, 1118–1129.

Grandvaux, N., tenOever, B. R., Servant, M. J. & Hiscott, J. (2002). The interferon antiviral response: from viral invasion to evasion. *Curr Opin Infect Dis* **15**, 259–267.

Gunther, S., Sommer, G., Plikat, U., Iwanska, A., Wain-Hobson, S., Will, H. & Meyerhans, A. (1997). Naturally occurring hepatitis B virus genomes bearing the hallmarks of retroviral G→A hypermutation. *Virology* **235**, 104–108.

Harris, R. S., Bishop, K. N., Sheehy, A. M., Craig, H. M., Pertersen-Mahrt, S. K., Watt, I. N., Neuberger, M. S. & Malim, M. H. (2003). DNA deamination mediates innate immunity to retroviral infection. *Cell* 113, 803–809.

Janini, M., Rogers, M., Birx, D. R. & McCutchan, F. E. (2001). Human immunodeficiency virus type 1 DNA sequences genetically damaged by hypermutation are often abundant in patient peripheral blood mononuclear cells and may be generated during near-simultaneous infection and activation of CD4(+) T cells. *J Virol* 75, 7973–7986.

Jarmuz, A., Chester, A., Bayliss, J., Gisbourne, J., Dunham, I., Scott, J. & Navaratnam, N. (2002). An anthropoid-specific locus of orphan C to U RNA-editing enzymes on chromosome 22. *Genomics* 79, 285–296.

Kobayashi, M., Takaori-Kondo, A., Shindo, K., Abudu, A., Fukunaga, K. & Uchiyama, T. (2004). APOBEC3G targets specific virus species. *J Virol* 78, 8238–8244.

Lecossier, D., Bouchonnet, F., Clavel, F. & Hance, A. J. (2003). Hypermutation of HIV-1 DNA in the absence of the Vif protein. *Science* 300, 1112.

Mangeat, B., Turelli, P., Caron, G., Friedli, M., Perrin, L. & Trono, D. (2003). Broad antiretroviral defence by human APOBEC3G through lethal editing of nascent reverse transcripts. *Nature* 424, 99–103.

Newman, E. N., Holmes, R. K., Craig, H. M., Klein, K. C., Lingappa, J. R., Malim, M. H. & Sheehy, A. M. (2005). Antiviral function of APOBEC3G can be dissociated from cytidine deaminase activity. *Curr Biol* 15, 166–170.

Noguchi, C., Ishino, H., Tsuge, M., Fujimoto, Y., Imamura, M., Takahashi, S. & Chayama, K. (2005). G to A hypermutation of hepatitis B virus. *Hepatology* 41, 626–633.

Norder, H., Courouce, A. M. & Magnius, L. O. (1994). Complete genomes, phylogenetic relatedness, and structural proteins of six strains of the hepatitis B virus, four of which represent two new genotypes. *Virology* 198, 489–503.

Peng, G., Lei, K. J., Jin, W., Greenwell-Wild, T. & Wahl, S. M. (2006). Induction of APOBEC3 family proteins, a defensive maneuver underlying interferon-induced anti-HIV-1 activity. *J Exp Med* 203, 41–46.

Rosler, C., Kock, J., Malim, M. H., Blum, H. E. & von Weizsacker, F. (2004). Comment on 'Inhibition of hepatitis B virus replication by APOBEC3G'. *Science* 305, 1403 (author reply 1403).

Rosler, C., Kock, J., Kann, M., Malim, M. H., Blum, H. E., Baumert, T. F. & von Weizsacker, F. (2005). APOBEC-mediated interference with hepadnavirus production. *Hepatology* 42, 301–309.

Samuel, C. E. (2001). Antiviral actions of interferons. *Clin Microbiol Rev* 14, 778–809.

Seeger, C. & Mason, W. S. (2000). Hepatitis B virus biology. *Microbiol Mol Biol Rev* 64, 51–68.

Sheehy, A. M., Gaddis, N. C., Choi, J. D. & Malim, M. H. (2002). Isolation of a human gene that inhibits HIV-1 infection and is suppressed by the viral Vif protein. *Nature* 418, 646–650.

Shindo, K., Takaori-Kondo, A., Kobayashi, M., Abudu, A., Fukunaga, K. & Uchiyama, T. (2003). The enzymatic activity of CEM15/Apobec-3G is essential for the regulation of the infectivity of HIV-1 virion but not a sole determinant of its antiviral activity. *J Biol Chem* 278, 44412–44416.

Shirakawa, K., Takaori-Kondo, A., Kobayashi, M., Tomonaga, M., Izumi, T., Fukunaga, K., Sasada, A., Abudu, A., Miyauchi, Y. & other authors (2006). Ubiquitination of APOBEC3 proteins by the Vif-Cullin5-ElonginB-ElonginC complex. *Virology* 344, 263–266.

Skalka, A. M. & Goff, S. P. (1993). *Reverse Transcriptase.* Cold Spring Harbor, NY: Cold Spring Harbor Laboratory Press.

Summers, J. & Mason, W. S. (1982). Replication of the genome of a hepatitis B-like virus by reverse transcription of an RNA intermediate. *Cell* 29, 403–415.

Suspene, R., Guetard, D., Henry, M., Sommer, P., Wain-Hobson, S. & Vartanian, J. P. (2005a). Extensive editing of both hepatitis B virus DNA strands by APOBEC3 cytidine deaminases in vitro and in vivo. *Proc Natl Acad Sci U S A* 102, 8321–8326.

Suspene, R., Henry, M., Guillot, S., Wain-Hobson, S. & Vartanian, J. P. (2005b). Recovery of APOBEC3-edited human immunodeficiency virus G→A hypermutants by differential DNA denaturation PCR. *J Gen Virol* 86, 125–129.

Tanaka, Y., Marusawa, H., Seno, H., Matsumoto, Y., Ueda, Y., Kodama, Y., Endo, Y., Yamauchi, J., Matsumoto, T. & other authors (2006). Anti-viral protein APOBEC3G is induced by interferon-α stimulation in human hepatocytes. *Biochem Biophys Res Commun* 341, 314–319.

Tsuge, M., Hiraga, N., Takaishi, H., Noguchi, C., Oga, H., Imamura, M., Takahashi, S., Iwao, E., Fujimoto, Y. & other authors (2005). Infection of human hepatocyte chimeric mouse with genetically engineered hepatitis B virus. *Hepatology* 42, 1046–1054.

Turelli, P., Jost, S., Mangeat, B. & Trono, D. (2004a). Response to comment of 'Inhibition of hepatitis B virus replication by APOBEC3G'. *Science* 305, 1403b.

Turelli, P., Mangeat, B., Jost, S., Vianin, S. & Trono, D. (2004b). Inhibition of hepatitis B virus replication by APOBEC3G. *Science* 303, 1829.

Wieland, S., Thimme, R., Purcell, R. H. & Chisari, F. V. (2004a). Genomic analysis of the host response to hepatitis B virus infection. *Proc Natl Acad Sci U S A* 101, 6669–6674.

Wieland, S. F., Spangenberg, H. C., Thimme, R., Purcell, R. H. & Chisari, F. V. (2004b). Expansion and contraction of the hepatitis B virus transcriptional template in infected chimpanzees. *Proc Natl Acad Sci U S A* 101, 2129–2134.

Wieland, S. F., Eustaquio, A., Whitten-Bauer, C., Boyd, B. & Chisari, F. V. (2005). Interferon prevents formation of replication-competent hepatitis B virus RNA-containing nucleocapsids. *Proc Natl Acad Sci U S A* 102, 9913–9917.

Wright, T. L. & Lau, J. Y. (1993). Clinical aspects of hepatitis B virus infection. *Lancet* 342, 1340–1344.

Zhang, H., Yang, B., Pomerantz, R. J., Zhang, C., Arunachalam, S. C. & Gao, L. (2003). The cytidine deaminase CEM15 induces hypermutation in newly synthesized HIV-1 DNA. *Nature* 424, 94–98.

PO Box 2345, Beijing 100023, China
www.wjgnet.com
wjg@wjgnet.com

World J Gastroenterol 2007 January 21; 13(3): 414-420
World Journal of Gastroenterology ISSN 1007-9327

RAPID COMMUNICATION

Clinical features and prognosis of patients with extrahepatic metastases from hepatocellular carcinoma

Kiminori Uka, Hiroshi Aikata, Shintaro Takaki, Hiroo Shirakawa, Soo Cheol Jeong, Keitaro Yamashina, Akira Hiramatsu, Hideaki Kodama, Shoichi Takahashi, Kazuaki Chayama

Kiminori Uka, Hiroshi Aikata, Shintaro Takaki, Hiroo Shirakawa, Soo Cheol Jeong, Keitaro Yamashina, Akira Hiramatsu, Hideaki Kodama, Shoichi Takahashi, Kazuaki Chayama, Department of Medicine and Molecular Science, Division of Frontier Medical Science, Programs for Biomedical Research, Graduate School of Biomedical Sciences, Hiroshima University, Hiroshima, Japan
Correspondence to: Kiminori Uka, MD, Department of Medicine and Molecular Science, Division of Frontier Medical Science, Programs for Biomedical Research, Graduate School of Biomedical Sciences, Hiroshima University, 1-2-3 Kasumi, Minami-ku, Hiroshima 734-8551, Japan. kiminori@hiroshima-u.ac.jp
Fax: +81-82-2575194
Received: 2006-10-29 Accepted: 2006-12-08

Abstract

AIM: To assess the clinical features and prognosis of 151 patients with extrahepatic metastases from primary hepatocellular carcinoma (HCC), and describe the treatment strategy for such patients.

METHODS: After the diagnosis of HCC, all 995 consecutive HCC patients were followed up at regular intervals and 151 (15.2%) patients were found to have extrahepatic metastases at the initial diagnosis of primary HCC or developed such tumors during the follow-up period. We assessed their clinical features, prognosis, and treatment strategies.

RESULTS: The most frequent site of extrahepatic metastases was the lungs (47%), followed by lymph nodes (45%), bones (37%), and adrenal glands (12%). The cumulative survival rates after the initial diagnosis of extrahepatic metastases at 6, 12, 24, and 36 mo were 44.1%, 21.7%, 14.2%, 7.1%, respectively. The median survival time was 4.9 mo (range, 0-37 mo). Fourteen patients (11%) died of extrahepatic HCC, others died of primary HCC or liver failure.

CONCLUSION: The prognosis of HCC patients with extrahepatic metastases is poor. With regard to the cause of death, many patients would die of intrahepatic HCC and few of extrahepatic metastases. Although most of HCC patients with extrahepatic metastases should undergo treatment for the primary HCC mainly, treatment of extrahepatic metastases in selected HCC patients who have good hepatic reserve, intrahepatic tumor stage (T0-T2), and are free of portal venous invasion may improve survival.

Key words: Hepatocellular carcinoma; Extrahepatic metastases; Prognosis; Causes of death

Uka K, Aikata H, Takaki S, Shirakawa H, Jeong SC, Yamashina K, Hiramatsu A, Kodama H, Takahashi S, Chayama K. Clinical features and prognosis of patients with extrahepatic metastases from hepatocellular carcinoma. *World J Gastroenterol* 2007; 13(3): 414-420

http://www.wjgnet.com/1007-9327/13/414.asp

INTRODUCTION

Hepatocellular carcinoma (HCC) is a highly malignant tumor with frequent intrahepatic metastasis. The prognosis of HCC patients has improved because of progress in therapeutic procedures, such as surgical resection, radiofrequency ablation (RFA), percutaneous ethanol injection (PEI), and transcatheter arterial chemoembolization (TACE)[1-3]. Moreover, progress in diagnostic modalities, such as ultrasonography (US), computed tomography (CT), magnetic resonance imaging (MRI), and digital subtraction angiography (AG) has led to a better detection of patients with early and small HCC or asymptomatic extrahepatic metastases.

The above improvements in survival and diagnostic modalities have resulted in increased detection of extrahepatic metastases from primary HCC and further increases are anticipated in the future. Several groups have investigated extrahepatic metastases from HCC, but many of such cases were in autopsy cases, in a small number of cases or case reports[4-15]. At present, the prognosis of patients with extrahepatic metastases from primary HCC is poor[16,17]. In this regard, there is only little information about the causes of death of such patients[18], and there is no consensus on the treatment strategy for extrahepatic metastases from HCC. For example, what treatment strategy should be used to treat intrahepatic HCC or extrahepatic metastases? Among patients with extrahepatic metastases from primary HCC, which patients should be treated? To our knowledge, there are no reports that

deal directly with these questions. In this relatively large study, we retrospectively assessed the clinical features and prognosis of 151 patients with extrahepatic metastases from primary HCCs, and described the treatment strategy for such patients.

MATERIALS AND METHODS

Patients

From June 1990 to December 2005, 995 consecutive patients with HCC were admitted to our hospital. Among these patients, 880 were initially diagnosed with HCC in our hospital while the others were treated previously for HCC in other hospitals. Extrahepatic metastases from primary HCC were detected in 151 (15.2%) of 995 patients. None of the patients was treated for extrahepatic metastases. All the 151 HCC patients with extrahepatic metastases (117 men and 34 women, median age: 64 years, range: 21-82 years) were enrolled in the present study.

Table 1 summarizes the clinical profile of the 151 patients at the initial diagnosis of extrahepatic metastases. These 151 patients were divided into groups A and B. Group A was consisted of 68 patients presented with extrahepatic metastases together with primary HCC at the initial diagnosis of HCC, group B was composed of 83 patients who received treatment for intrahepatic HCC, and developed extrahepatic metastases during the follow-up period. Among them, 37 (25%) patients were treated previously for primary HCC in other hospitals, 90 patients were of performance status (PS) of 0, 43 patients of 1, 9 patients of 2, 6 patients of 3, and 3 patients of 4[19]. The etiology of the background liver disease was hepatitis B virus (HBV) in 33 patients, hepatitis C virus (HCV) in 89 patients, HBV and HCV in 5 patients, and non-B non-C in 24 patients. The hepatic reserve was Child-Pugh grade A in 88 patients, grade B in 48 patients, and grade C in 15 patients. We evaluated the primary tumor stage according to the Liver Cancer Study Group of Japan criteria[20], based on the following three conditions (T factor): solitary, < 2 cm in diameter, and no vessel invasion. T1 was defined as fulfilling the three conditions, T2 as fulfilling two of the three conditions, T3 as fulfilling one of the three conditions, T4 as fulfilling none of the three conditions. The primary HCC tumor stage at the first diagnosis of extrahepatic metastases was T0 (no intrahepatic HCC) in 11 (7%) patients, T1 in 4 (3%) patients, T2 in 13 (9%) patients, T3 in 43 (28%) patients, and T4 in 80 (53%) patients. Twenty seven of 28 patients with intrahepatic tumor stage T0-T2 were treated previously for intrahepatic HCC. The median size of the main intrahepatic primary tumor was 48 mm (range, 0-160 mm). Intrahepatic tumor morphology was nodular type in 83 (55%) patients, non-nodular type in 57 (38%) patients, and no intrahepatic HCC in 11 (7%) patients. Table 1 lists the sites of extrahepatic metastases at enrollment. Among the 151 patients with extrahepatic metastases, the sites of metastases were the lungs in 63 patients, lymph nodes in 60 patients, bones in 51 patients, adrenal glands in 16 patients and other locations (e.g., peritoneum, pancreas and nasal passages). In some patients, two or more distant metastatic tumors were found in one or more organs.

Table 1 Clinical profile of 151 HCC patients with extrahepatic metastases at the initial diagnosis of extrahepatic metastases

Age (yr)	64 (21-82)
Sex (male/female)	117/34
Etiology (HBV/HCV/HBV + HCV/others)	33/89/5/24
PS (0/1/2/3/4)	90/43/9/6/3
Intrahepatic tumor stage (T0/1/2/3/4)	11/4/13/43/80
Intrahepatic main tumor size (mm)	48 (0-160)
Intrahepatic tumor volume (< 50%/≥ 50%)	103/48
Intrahepatic tumor morphology (nodular type/non nodular type/no intrahepatic HCC)	83/57/11
Grade of portal vein invasion (Vp 0/1/2/3/4)	74/0/26/28/23
Child-Pugh grade (A/B/C)	88/48/15
AFP (ng/mL)	741.8 (< 5-861600)
DCP (mAU/mL)	1300 (< 10-391400)
Site of extrahepatic metastases, *n* (%)	
Lung	63 (42)
Lymph nodes	60 (40)
Bone	51 (34)
Adrenal	16 (11)
Peritoneum	1 (0.7)
Pancreas	1 (0.7)
Nasal passages	1 (0.7)

Data are expressed as medians and ranges unless indicated otherwise. HBV: hepatitis B virus; HCV: hepatitis C virus; PS: Eastern Cooperative Oncology Group performance status; T0: no intrahepatic HCC; Portal invasion assessed Vp1: tumor thrombus in a third or more of the peripheral branches; Vp2: in the second branch; Vp3: in the first branch; Vp4: in the trunk; AFP: alpha-fetoprotein; DCP: Des-γ-carboxy prothrombin.

Hepatocellular carcinoma

A definitive diagnosis of HCC was based on the finding of typical hypervascular radiological features or histopathological examination of needle biopsy specimen. HCC was also assessed by US, CT, and/or AG. Furthermore, CT was obtained during arterial portography and computerized tomographic hepatic arteriography. Further assessment of HCC was conducted by measuring α-fetoprotein (AFP) and des-γ-carboxy prothrombin (DCP).

Extrahepatic metastases were diagnosed by CT, MRI, bone scintigraphy, X-ray, and/or positron emission tomography (PET) with ^{18}F-fluorodeoxyglucose (FDG), or diagnosed by histopathological examination of surgically resected specimen or biopsy. When we suspected extrahepatic metastases with HCC, we always ruled out other malignancies (such as gastric cancer, colon cancer and lung cancer) by several imaging modalities, serological tumor markers and/or pathological examination.

Follow-up

All the 151 HCC patients with extrahepatic metastases were followed up during the observation period and no one was lost to follow-up. The median follow-up period was 4.9 mo (range, 1-37 mo). After the diagnosis of HCC, all patients were screened at regular intervals for the development of intra/extra hepatic metastases by clinical examination, AFP, DCP, and/or various imaging modalities. Serological tumor markers were measured once every month. US, CT or MRI was performed once every three to six months.

Statistical analysis and ethical considerations

Differences between groups were examined for statistical significance using the Mann-Whitney test (*U*-test) and χ^2 test where appropriate. Cumulative survival rate was assessed by the Kaplan-Meier life-table method and the differences were evaluated by the log rank test. The following 15 potential predictors were assessed in this study: PS (0 *vs* 1-4), age (≤ 65 *vs* > 65 years), sex (M *vs* F), Child-Pugh stage (A *vs* B, C), intrahepatic tumor stage (T0-T2 *vs* T3, T4), main intrahepatic tumor size (≤ 50 *vs* > 50 mm), intrahepatic tumor volume (≤ 50% *vs* > 50%), intrahepatic tumor morphology (nodular type *vs* non nodular type), portal venous invasion (Vp 0-2 *vs* > Vp 3, 4), AFP (≤ 400 ng/mL *vs* > 400 ng/mL), DCP (≤ 1000 mAU/mL *vs* > 1000 mAU/mL), site of extrahepatic metastases (lung *vs* others, bone *vs* others, only lymph node *vs* others), and treatment for extrahepatic metastases (performed *vs* not performed). All factors that were at least marginally associated with the survival after diagnosis of extrahepatic metastases ($P < 0.05$) were entered into a multivariate analysis. The hazard ratio and 95% confidence interval (95% CI) were calculated to assess the relative risk confidence. All analyses described above were performed using the SPSS program (version 11.0, SPSS Inc., Chicago, IL).

The study protocol was approved by the Human Ethics Review Committee of Graduate School of Biomedical Sciences, Hiroshima University and a signed consent form was obtained from each patient.

RESULTS

Site of extrahepatic metastases

Table 2 lists the sites of extrahepatic metastases identified throughout the follow-up period. The most frequent site of metastases that were identified throughout the follow-up period was the lung (n = 71 patients, 47%), followed by lymph nodes (n = 68 patients, 45%), bone (n = 56 patients, 37%), and adrenal glands (n = 18 patients, 12%). Brain metastases were identified in 2 (1%) patients. One (0.7%) patient each had metastases in the peritoneum, pancreas, nasal passages, muscle, skin, diaphragm, and colon. Autopsy was performed in 14 cases with metastases. Despite the detection of extrahepatic metastases in these 14 patients before autopsy, additional extrahepatic metastases were detected on postmortem examination (lymph nodes, diaphragm, and colon). At the first diagnosis of extrahepatic metastases, 109 (72%) patients had single-organ metastases, while the others had multiple organ metastases.

Among the 71 patients with lung metastases, 23 patients had bilateral lung metastases, 14 had additional extrapulmonary site of metastatic disease. The size of pulmonary nodules ranged from 9 to 30 mm at initial diagnosis of extrahepatic HCC. Few patients had symptoms (cough, dyspnea, and pleural effusion) related to lung metastases, and 8 patients who had severe symptoms died subsequently of respiratory failure. The median survival period of these 8 patients was 4.3 mo (range, 2.5-14.4 mo).

Table 2 Sites of extrahepatic HCC detected throughout the entire follow-up period

Site	Patients (n = 151), n (%)
Lung	71 (47)
Lymph nodes	68 (45)
Bone	56 (37)
Adrenal	18 (12)
Brain	2 (1)
Peritoneum	1 (0.7)
Pancreas	1 (0.7)
Nasal	1 (0.7)
Muscle	1 (0.7)
Skin	1 (0.7)
Diaphragm	1 (0.7)
Colon	1 (0.7)

Among the 68 patients with lymph node metastases, metastases were identified in 64 regional lymph nodes. The most common site was in the paraaortic nodes (31/64), followed by portohepatic nodes (21/64), periceliac nodes (6/64) and peripancreatic nodes (6/64). The majority of patients with regional lymph nodes metastases were asymptomatic, but few regional lymph nodes (portohepatic nodes) caused obstructive jaundice. Distant nodal metastases were found at 17 sites. The most common site was the mediastinum nodes (10/17), followed by subclavicular nodes (3/17), iliac nodes (2/17), cardiophrenic node (1/17), and retrocrural node (1/17). All distant lymph node metastases were not associated with clinical symptoms in this study.

Fifteen of 56 patients with bone metastases had multiple bone metastases at the initial diagnosis of bone metastases. The total number of bone metastatic sites was 88. The most frequent site was the vertebra (63/88; cervical vertebrae = 9, thoracic vertebrae = 38, and lumbar vertebrae = 16), followed by the ribs (8/88). Bone metastases were diagnosed by CT, MRI, bone scintigraphy, and/or PET with FDG.

Of the 18 patients with adrenal gland metastases, 13 had right adrenal gland metastases, 4 had left adrenal gland metastases and only one patient had bilateral metastases. These metastases were not associated with symptoms.

Treatments of extrahepatic metastases

All patients with Child-Pugh grade other than C or PS other than 2-4 were treated for intrahepatic HCC, and many of them were continuously treated after the diagnosis of extrahepatic metastases. On the other hand, HCC patients with Child-Pugh grade C or PS of 2-4 received supportive care. Forty-nine (32%) of 151 patients were treated for extrahepatic metastases by surgical resection, TACE, systemic chemotherapy, and/or radiotherapy. The 49 patients had extrahepatic metastases that were considered to worsen prognosis.

Surgical resection was performed in three (2%) patients (with regional lymph node, adrenal gland and lung metastases). The survival periods after surgical resection of extrahepatic metastases were 7 mo (in patients with lymph node metastases), 23 mo (in patients adrenal gland metastases), and 37 mo (in patients with lung metastases).

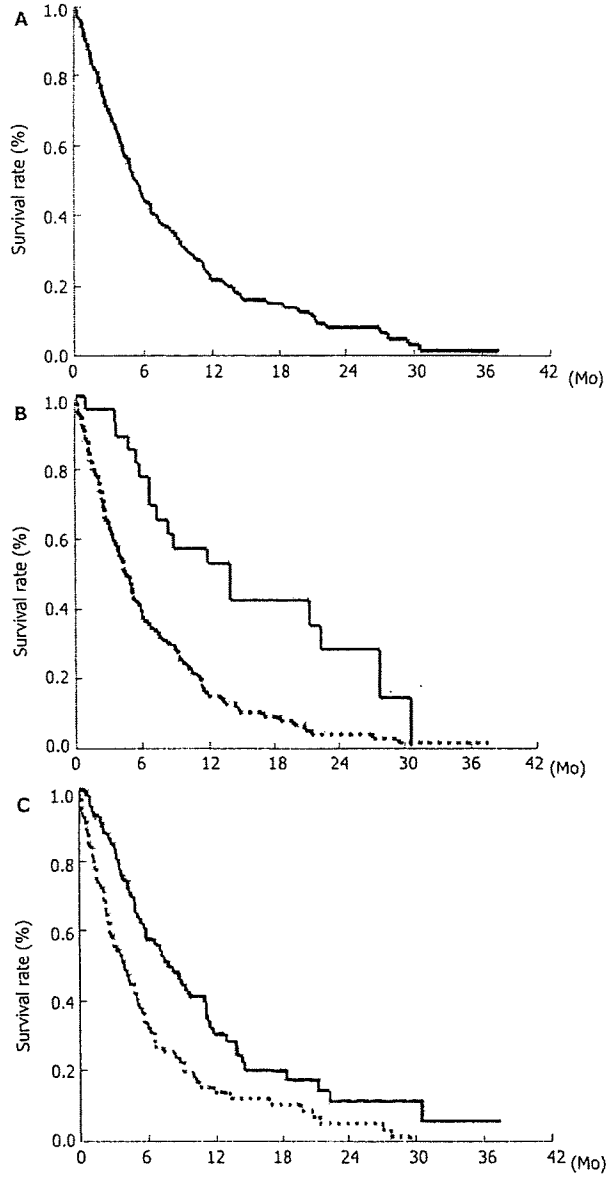

Figure 1 Survival rate of 151 HCC patients with extrahepatic metastases (A), intrahepatic tumor stage (B) [solid line: T0-T2, dashed line: T3, T4 (log-rank test: $P < 0.001$)], and after treatment of extrahepatic metastases (C) [solid line: treatment group, dashed line: no treatment group (log-rank test: $P < 0.001$)].

These three were all alive without recurrence of extrahepatic metastases during the observation period. In each of these 3 patients, hepatic reserve was Child-Pugh stage A, no intrahepatic HCC was not detected, and PS was 0.

TACE was performed in 8 (5%) patients (7 patients with adrenal gland metastases, and one patient with paraaortic lymph node metastases). Systemic chemotherapy was used in 39 (26%) patients. Chemotherapy included 5-fluorouracil, carboplatin, cisplatin. Twenty-five of the 39 patients had lung metastases, 10 had lymph node metastases, 2 had bone metastases, one had lung and lymph node metastases, and one had lung, adrenal gland and lymph node metastases.

Radiotherapy was performed in 36 (24%) patients.

Table 3 Univariate analysis of predictors of survival after initial diagnosis of extrahepatic metastases in 151 patients

Variable	Hazard Ratio	95% CI	*P*
PS (0 *vs* 1-4)	2.181	1.50-3.17	< 0.001
Age (≤ 65 *vs* > 65 yr)	0.988	0.97-1.0	0.18
Sex (M *vs* F)	0.889	0.57-1.38	0.601
Child Pugh stage (A *vs* B, C)	2.323	1.73-3.12	< 0.001
Intrahepatic main tumor size (≤ 50 *vs* > 50 mm)	2.321	1.52-3.54	< 0.001
Intrahepatic tumor volume (≤ 50 *vs* > 50%)	2.523	1.71-3.72	< 0.001
Intrahepatic tumor morphology (nodular *vs* non nodular)	1.506	1.04-2.18	0.03
Vp (0-2 *vs* 3, 4)	2.247	1.53-3.29	< 0.001
AFP (≤ 400 *vs* > 400 ng/mL)	1.158	0.80-1.68	0.439
DCP (≤ 1000 *vs* > 1000 mAU/mL)	1.584	1.08-2.33	0.02
Treatment (performed *vs* not performed)[1]	2.385	1.51-3.77	< 0.001
Site (lung *vs* others)[2]	1.065	0.74-1.52	0.731
Site (bone *vs* others)	1.61	1.11-2.33	0.012
Site (only lymph node *vs* others)	1.133	0.74-1.74	0.567

[1]Treatments: various treatments for extrahepatic metastases (surgical resection, TACE, systemic chemotherapy and/or radiotherapy); [2]Site: site of extrahepatic metastases.

Curative therapy was performed in 10 patients (6 patients with lymph node metastases and 4 patients with adrenal gland metastases). Palliative therapy was performed in the remaining 26 patients who had severe pain due to bone metastases. Furthermore, 9 patients with painful bone metastases were treated with RFA therapy combined with cementoplasty[21]. Nonsteroidal anti-inflammatory drugs or opioids were used in patients with bone metastases due to severe pain.

Survival data

The cumulative survival rates of the 151 HCC patients with extrahepatic metastases after initial diagnosis of extrahepatic metastases at 6, 12, 24, and 36 mo were 44.1%, 21.7%, 14.2%, and 7.1%, respectively (Figure 1A). The median survival period was 4.9 mo (range, 1-37 mo). Survival was compared among patients with intrahepatic tumor stage T0-T2 and T3, T4 (Figure 1B). The rate was significantly higher in the intrahepatic tumor stage T0-T2 groups than in the T3, T4 groups ($P < 0.001$). We investigated the determinants of survival after initial diagnosis of extrahepatic metastases. Univariate analysis identified the following 9 factors significantly influencing survival: PS, 0 ($P < 0.001$); Child-Pugh grade, A ($P < 0.001$); intrahepatic main tumor size, < 50 mm ($P < 0.001$); intrahepatic tumor volume, < 50% ($P < 0.001$); portal venous invasion, Vp 0-2 ($P < 0.001$); use of treatment for extrahepatic metastases ($P < 0.001$, Figure 1C); bone metastasis ($P = 0.012$); DCP < 1000 mAU/mL ($P = 0.02$); and nodular type intrahepatic tumor ($P = 0.03$) (Table 3). Since the variables could be mutually correlated, multivariate analysis was performed. The analysis identified the following four variables as significant and independent determinants of survival after initial diagnosis of extrahepatic metastases: PS ($P < 0.001$), portal venous invasion ($P < 0.001$), treatment of extrahepatic metastases ($P = 0.003$), and Child-Pugh grade ($P = 0.009$) (Table 4).

Table 4 Multivariate analysis of predictors of survival after initial diagnosis of extrahepatic metastases among 151 patients

Variable	Hazard ratio	95% CI	P
PS (0 *vs* 1-4)	5.576	2.431-12.152	< 0.001
Vp (0-2 *vs* 3, 4)	4.792	2.137-10.712	< 0.001
Treatment (performed *vs* not performed)	4.134	1.539-11.011	0.003
Child pugh stage (A *vs* B, C)	2.372	1.247-4.914	0.008

Causes of death

Twenty-five patients were still alive at the end of this study while 126 patients died. Of the latter group, intrahepatic tumor stages at the first diagnosis of extrahepatic metastases were T0-2 in 17 patients and T3-4 in 109 patients. One hundred and twelve (89%) patients died of intrahepatic HCC or liver failure. Fourteen (11%) patients died of extrahepatic HCC (Table 5). Eight patients died of respiratory failure due to lung metastases. Four patients died of bone metastases-related disease. Two patients died of obstructive jaundice due to portohepatic node metastasis.

Of the 4 patients who died of bone metastases-related disease, 3 died of intracranial hypertension due to skull metastasis. Another patient died of vertebra metastasis-related disease. He was 69-year old at first diagnosis of bone metastases. He suffered from complete spinal cord injury due to vertebral metastasis with gradual worsening of PS. Finally, PS changed to 4 and the patient died of aspiration-related pneumonia. The survival period after first diagnosis of extrahepatic metastases was 11.5 mo.

Among the 14 patients who died of extrahepatic HCC, 3 had chronic hepatitis, 7 had cirrhosis of Child-Pugh grade A, 3 had cirrhosis of Child-Pugh grade B, and 1 had cirrhosis of Child-Pugh grade C. All patients who died of extrahepatic HCC with the exception of that with Child-Pugh grade C had some hepatic reserve until death. Intrahepatic tumor stage at first diagnosis of extrahepatic metastases was T0 (3 patients), T1 (4 patients), T2 (1 patient), T3 (5 patients), and T4 (1 patient). All 8 patients with intrahepatic tumor stage T0-T2 were treated previously for intrahepatic HCC. Eight of 17 (47%) patients with intrahepatic tumor stage T0-T2 died of extrahepatic metastases. On the other hand, 6 of 109 (6%) patients with intrahepatic tumor stages T3 and T4 died of extrahepatic metastases. The mortality rate of patients with intrahepatic tumor stage T0-T2 was significantly higher than that of patients with intrahepatic tumor stages T3 and T4 ($P = 0.001$) (Table 6).

Table 5 Clinical profile of 14 patients who died of extrahepatic metastases during the follow-up period

Case	Presentation	Site	Intrahepatic HCC stage	Sex	Age (yr)	Child-Pugh stage	Etiology
1	R	Lung	T3	M	65	A	HCV
2	R	Lung	T4	M	35	CH	HBV
3	R	Lung	T3	M	56	A	HBV
4	R	Lung, vertebra	T0	M	40	CH	HBV
5	R	Lung, vertebra	T1	M	69	A	HBV
6	R	Lung, LN	T0	M	63	B	HBV
7	R	Lung, vertebra, nasal	T0	M	50	A	HBV
8	R	Lung	T3	M	73	A	NBNC
9	I	Skull	T1	M	57	A	HCV
10	I	Skull	T2	F	72	C	HCV
11	I	Skull	T3	M	56	B	HCV
12	A	Vertebra	T3	M	69	A	HCV
13	O	Lung, rib, LN	T1	M	74	A	HCV
14	O	Vertebra, LN	T1	M	70	B	HCV

All patients with intrahepatic tumor stage T0-T2 were treated previously for intrahepatic HCC. R: respiratory failure; CH: chronic hepatitis; LN: lymph node; NBNC: no hepatitis B virus or hepatitis C virus; I: intracranial hypertension symptom; A: aspiration-related pneumonia; O: obstructive jaundice.

Table 6 Causes of death of 126 HCC patients with extrahepatic metastases

Intrahepatic tumor stage	Intrahepatic HCC or liver failure	Extrahepatic HCC
T0-2 ($n = 17$)	53% (9/17)	47% (8/17)
T3-4 ($n = 109$)	94% (103/109)	6% (6/109)

DISCUSSION

The prognosis of HCC patients with extrahepatic metastases is unsatisfactory[16,17] and often not well known[18]. In the present study, we assessed the clinical features and prognosis of 151 consecutive HCC patients with extrahepatic metastases. The incidence of extrahepatic metastases from HCC was 15.2%. The most frequent metastatic sites were the lung, lymph nodes, bone, and adrenal gland. The cumulative survival rates of the 151 patients after the initial diagnosis of extrahepatic metastases at 6, 12, 24, and 36 mo were 44.1%, 21.7%, 14.2%, 7.1%, respectively. The median survival period was 4.9 mo (range, 1-37 mo). The mortality rate due to extrahepatic metastases from HCC was 11% (14/126).

Extrahepatic metastases have been reported to occur in 13.5%-42% of HCC patients[22-24]. In this study, the prevalence of extrahepatic metastases was 15.2%. Though we screened all HCC patients at regular intervals for intra/extra hepatic metastases, not all patients received a full metastatic follow up based on the use of several diagnostic techniques. Since the majority of HCC patients with extrahepatic metastases were asymptomatic, it is possible to miss asymptomatic metastases such as those in the lungs, distant lymph nodes, muscles and rectum.

Based on the initial diagnosis of intrahepatic HCC, Natsuizaka *et al*[16] reported that patients with advanced HCC develop extrahepatic metastases significantly more frequently than those with less advanced HCC. At the initial diagnosis of extrahepatic metastases, many HCC patients with extrahepatic metastases have been reported